J Math Chem (2010) 48:187–223
DOI 10.1007/s10910-010-9660-z

ORIGINAL PAPER

# Approximate symmetry characteristics using fuzzy-subset theory study for chiral transitions of allene-1,3,-dihalides

**Xuezhuang Zhao · Zhenfeng Shang · Zucheng Li · Xiufang Xu · Guichang Wang · Ruifang Li · Yun Li**

Received: 16 February 2009 / Accepted: 22 January 2010 / Published online: 18 February 2010


**Abstract** Based on our study of the application of fuzzy-subset theory to the characterization of imperfect symmetry in some stable molecular systems and simple dynamic molecular systems, we analyze the internal rotation process of allene-1,3-dihalides. Allene-1,3-dihalides (CHX=C=CHY, where X and Y may be the same or different halogen atoms) are optically chiral nonplanar molecules. The two end-groups may internally rotate about the near straight linear C=C=C axis, and the molecule may change its chirality. The internal rotation process may pass through two different planar transition state (TS): *cis*-TS and *trans*-TS, which belong to $C_{2v}$ and $C_{2h}$ point groups (as X and Y to be same), respectively. The intrinsic reaction coordinate (IRC) corresponding to the two TS processes is denoted as *cis*-IRC and *trans*-IRC. However, for the whole IRC reaction process, only their subgroup $C_2$ well-defined symmetry remains. Other symmetry transformations in $C_{2v}$ and $C_{2h}$ point groups can only be examined in terms of imperfect symmetry, although there appear certain reaction reversal joint point group $G(R_cC_{2v})$ and $G(R_tC_{2h})$ well-defined symmetry in the dynamics through the IRC processes. If X and Y are different, the stable molecule has no conventional nontrivial point group symmetry. The internal rotation processes may pass through two different planar TS's (*cis*-and *trans*-TS). The TS will still be a planar molecule belonging to $C_S$ point group with the molecule plane as its symmetry plane. Other states in the IRC may belong to certain reaction reversal joint point groups, $G(RM)_C$ and $G(RM)_T$. We have thus examined the approximate symmetry of MO's related to $C_2$ point group. Moreover, we have also analyzed the membership

X. Zhao (✉) · Z. Shang · X. Xu · G. Wang · R. Li · Y. Li
Department of Chemistry, Nankai University, 300071 Tianjin, People's Republic of China
e-mail: zhaoxzh@nankai.edu.cn

Z. Li
Center for Theoretical and Computational Chemistry, Nankai University, 300071 Tianjin, People's Republic of China

functions, representation components, and their relationships shown in the MO fuzzy main representation correlation diagrams.

**Keywords** Fuzzy subset · Allene dihalides · Chiral transition · MO fuzzy correlation diagram

## 1 Introduction

In theoretical chemistry, some important results of fuzzy subset theory in relation to the approximate symmetry have been obtained [1–11]. In which those by P. G. Mezey and his coworkers are particularly important. In our previous studies, in addition to this field in connection to such approximate symmetry (sometimes, we called it fuzzy symmetry) of some stable molecules and their molecule orbitals (MO's) [12–17], we have also succinctly analyzed the simple tri-atom linear dynamic systems [18] and the internal rotation process of propadine (allene) [19]. In this paper, the chiral transition process of the molecular internal rotation of allene-1,3-dihalides as a prototype will be analyzed in detail. This process is distinct from that of allene whose four identical H atoms link to the molecular axis, and whose initial and final state in the rotation will be the same, and the intrinsic reaction coordinate (IRC) and transition state (TS) due to clockwise or anticlockwise rotation are also the same.

However, these are not true for allene-1,3-dihalides (CHX=C=CHY) because the 1,3-H atoms in allene are substituted by halogen atoms; the stable molecules will be a pair of enantiomers, regardless of the two halogens X and Y being the same or not. On the other hand, IRC and TS related to clockwise or anticlockwise rotation are different. The TS leads to *cis*- or *trans*-configuration (X and Y are on the same or different sides of the C=C=C axis), will be denoted as *cis*-TS or *trans*-TS, respectively. The relative symmetry characteristics for *cis*-IRC and *trans*-IRC in the entire internal rotation process are derived from those of allene, although the C=C=C axis of dihalides slightly deviate from the straight line in allene. Through the internal rotation process, the two CHX groups in the molecule will rotate simultaneously but not about the same straight C=C=C axis. Some well-defined symmetry of allene will degenerate to imperfect one. Such imperfect symmetry of allene-1,3-dihalides may affect its MO irreducible representation component. We will examine this point farther along with the corresponding MO fuzzy correlation diagrams of the processes and the relationship between the MO membership function and the irreducible representation component in this paper. The symmetry in relation to the reaction reversal joint point group will also be analyzed here.

## 2 Molecular geometry and computation details

### 2.1 Molecular geometry

The simplest cumulated diene is 1,2-propadiene, $CH_2$=C=$CH_2$, *i.e.* allene. The central carbon in such compounds is *sp*-hybridized (with only two bonding partners), and so the double bond array is linear. Since the $\pi$-bonds of allenes are orthogonal,

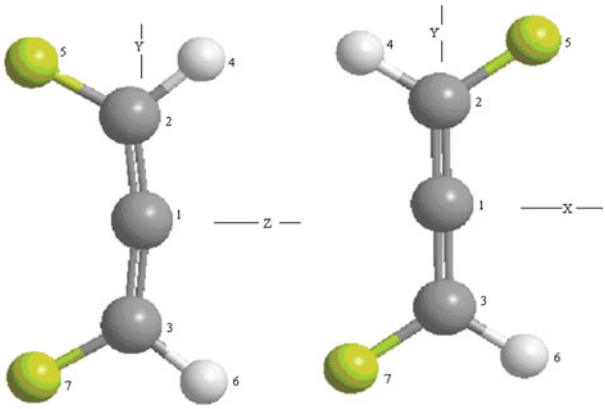


**Fig. 1** Two transition states for the internal rotation process of allene-1,3-dihalides (CHX=C=CHY), at AM1 level

the planes defined by the end carbon substituents are also orthogonal. As the end hydrogen atoms of allene are substituted by various atoms or groups, the derivative will be chiral. Recently, there are some interesting research on the derivative and the asymmetric chemistry [20]. Therefore, the chiral transition of these molecules in the internal rotation can also be important. The stable configuration of allene will be non-planar cross-shaped, while the planar configuration will be of the higher energy [21], corresponding to the TS of the internal rotation [19]. For allene molecule, the internal rotation does not accompany chiral transition, but for allene-1,3-dihalides the rotation may accompany chiral transition.

When allene-1,3-dihalides undergoes chiral transition in internal rotation, the atomic numbering and adjacent relationship may be defined as follows: 1, 2 and 3 denote three C atoms while 1 numbers the mid-C atom as C(1). Other atoms are numbered similarly; 4 and 6 number the two H atoms, and 5 and 7 number the two halogen atoms. H(4) and X(5) are assigned to bind C(2), but H(6) and Y(7) to C(3).

In this paper all calculations are at AM1 level using the Gaussian program [22]. To start with, we calculate the TS of the internal rotation of allene-1,3-dihalides. As shown in Fig. 1, there are two different TS for each allene-1,3-dihalide, *cis*-TS and *trans*-TS.

Both TS's are planar. If the two halogen atoms are the same, the *cis*-TS belongs to $C_{2v}$ and the *trans*-TS to $C_{2h}$. The corresponding IRC may be denoted as *cis*-IRC and *trans*-IRC, respectively. The two-fold rotation ($C_2$) axis, which remains in the whole internal rotation, is chosen as the Z axis, and the direction connecting C(2) and C(3) as the Y axis. Therefore, the *cis*-TS is in the YZ-coordinate plane, and so is the two-fold axis, but the *trans*-TS is in the XY-coordinate plane whereas $C_2$ axis is perpendicular to this plane. The origin of Cartesian coordinate system may be chosen at C(1), the midpoint of the connecting line between C(2) and C(3) if the halogen atoms X and Y are the same and both denoted as V. If the two halogen atoms are different, although these two TS's will still be planar, but the $C_2$ symmetry will not present in the whole

process. In addition, the C=C=C skeleton may somewhat deviate from a straight line, yet we will still choose the Cartesian coordinate system as above. Certainly, the $C_2$ axis will be replaced by a fuzzy $C_2$ axis, i.e. the relative two-fold rotation symmetry transformation with the membership function less one. It is notable that, according to the standard orientation in Gaussian program, the directions of Z- and other axes of the *cis*-TS and *trans*-TS with $C_{2v}$ and $C_{2h}$ symmetry coincide those chosen above, whereas the directions of TS's without such well-defined symmetry, such as in the cases of TS with different halogen atoms, may not coincide. In the calculation of IRC's, we use the standard orientations of Gaussian program. The above chosen Cartesian coordinate system is only necessary of the calculation of the MO representation component.

Two TS's and corresponding two IRC's, *cis*-IRC and *trans*-IRC, are obtained. According to the calculation, we also obtained the allene-1,3-dihalide skeleton configuration of certain single points alone the IRC. However, to research on the fuzzy subset theory for symmetry, we need to examine a pair of molecular configurations with the opposite IRC values (e.g., IRC equal $x$ and $-x$). However, from the Gaussian program, we cannot locate such configurations directly, so we used the linear interpolation method. We may then obtain the pair molecular configurations with the opposite values of IRC, one by one. Sometimes, however, we must change the Gaussian standard orientation to another one as chosen above. The geometric configuration, Cartesian coordinate system and atomic numbering of allene-1,3-dihalides for the whole IRC process are shown in Fig. 2, where the origin is set at C(1) as described above. In such Cartesian coordinate system, the $C_2$ axis (for two same halogens) or fuzzy $C_2$ axis (for different halogens) points to the $Z$-axis direction. Interestingly, if we set the $C_2$ axis along the $X$-direction, which is allowed, the $C_2$ transformation rule for the $p$-MO's parallel to the $C_2$ axis and that for perpendicular to the $C_2$direction are different. As shown in Fig. 2, this corresponds to the *cis*-IRC path, and it is similar for the *trans*-IRC path (omitted here). It should be noted that the Z-matrix for a certain molecular configuration should be the same for different choices of the Cartesian coordinate system.

Using the Gaussian program [22], we obtained the point-by-point molecular configurations including TS's and two stable molecules along the IRC. The stable allene-1,3-dihalides are a pair of enantiomers (Fig. 3). For *cis*- and *trans*-IRC, the pair of enantiomers are the same. The stable molecule with same halogen atoms, (V= X=Y) should belong to the $C_2$point group, but that with different X and Y should not. The coordinate systems in Figs. 2 and 3 are the same. These enantiomers may have well-defined mirror reflection symmetry, each other.

## 2.2 Space factor and intrinsic factor

Now we consider allene-1,3-dihalides with the same halogens. To start with, we analyze *cis*-IRC in which the corresponding *cis*-TS with the higher symmetry $C_{2V}$; as H and halogen atoms deviate from the *cis*-TS molecular plane other states will have lower $C_2$ symmetry, as well:

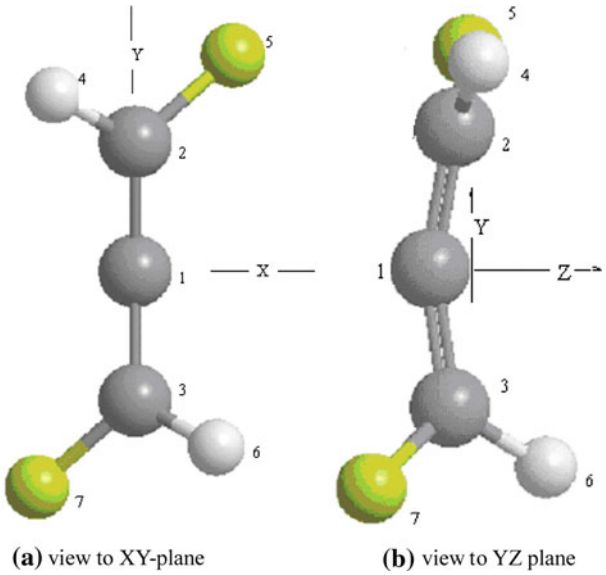


**(a)** view to XY-plane **(b)** view to YZ plane

**Fig. 2** Coordinate system and atomic numbering of allene-1,3-dihalides (CHX=C=CHY) in internal rotation process

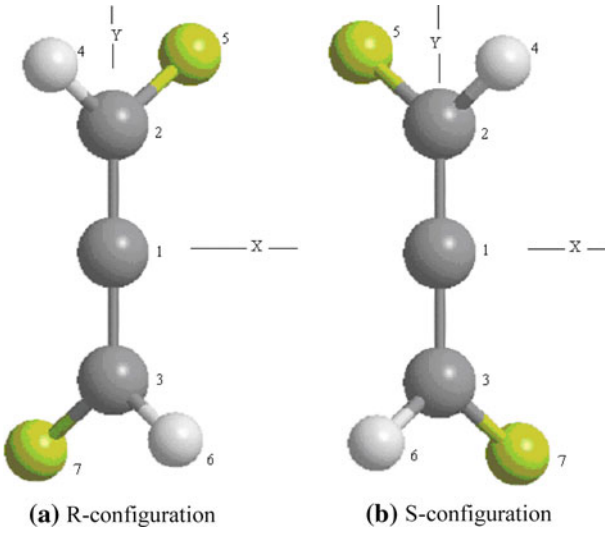


**(a)** R-configuration **(b)** S-configuration

**Fig. 3** The stable molecules of allene-1,3-dihalides (product and reactant of internal rotation) are a pair of the optical enantiomers. (at AM1 level), where **a** and **b** are R- and S-configuration (Newman projection), respectively

$$C2 : G_{cis-\mathrm{IRC}} = \left\{\hat{E}, \hat{C}_2\right\} \tag{1a}$$

$$C_{2V} : G_{cis-\mathrm{TS}} = G_{cis-\mathrm{IRC}} \cup G'_{cis-\mathrm{TS}} = \left\{\hat{E}, \hat{C}_2\right\} \cup \left\{\hat{M}_{XZ}, \hat{M}_{YZ}\right\}$$
$$= \left\{\hat{E}, \hat{C}_2, \hat{M}_{XZ}, \hat{M}_{YZ}\right\} \tag{1b}$$

Through both *cis*-IRC and *trans*-IRC belong to $C_2 = G_{\mathrm{IRC}} = \left\{\hat{E}, \hat{C}_2\right\}$ group, the $G_{\mathrm{TS}}$ has an additional symmetry related to mirror reflections, $G'_{\mathrm{TS}} = \left\{\hat{M}_{XZ}, \hat{M}_{YZ}\right\}$. Except for the *cis*-TS, all other states in the *cis*-IRC do not have the symmetry related to $G'_{\mathrm{TS}} = \left\{\hat{M}_{XZ}, \hat{M}_{YZ}\right\}$, but have the symmetry in relation to the joint transformations, $\hat{R}\hat{M}_{XZ}$ and $\hat{R}\hat{M}_{YZ}$, where $\hat{R}$ is the reaction reversal transformation whose operation makes the IRC value of a certain state to its opposite value of another state [23,24]. Such symmetry exists along the whole *cis*-IRC, so all the membership functions of $\hat{E}$, $\hat{C}_2$, $\hat{R}\hat{M}_{XZ}$ and $\hat{R}\hat{M}_{YZ}$ should be equal one. Meanwhile, for the *cis*-IRC states other *cis*-TS, we may analyze the approximate symmetry in relation to the transformations in $G'_{\mathrm{TS}} = \left\{\hat{M}_{XZ}, \hat{M}_{YZ}\right\}$. It should be pointed out that for an approximate symmetry system the operation of one simple transformation $G'_{\mathrm{TS}} = \left(\hat{M}_{XZ} \text{ or } \hat{M}_{YZ}\right)$ may change some atom (*e. g.* J-atom) to a position $G^{\#}J$ without any atom. Although we may choose GJ-atom near $G^{\#}J$ [12–19], certainly some approximation will thus be introduced. The different atomic positions would affect the LCAO-MO coefficient, and then the atomic criteria and the membership functions will somewhat be adjusted. In this way, we analyze the stable molecule to find the satisfactory results.

As the alteration of atomic positions of the dynamic system is small in relation to those of a certain key state, the change of the properties would also be small. If the atomic criterion is invariant towards the atomic position, then the above method would not be useful. Therefore, we use the above method to analyze the imperfection of MO's symmetry, but not to that of molecular skeleton for which the invariant atomic numbers are used as the criterion. For example, we analyzed the polyyne [17], indicating that the difference between single- and tri- bonds did present in the membership function of MO's, but not of skeleton. For a dynamic system, in additional to the intrinsic factor of the atomic criterion, we will also examine how the spatial factor affects the molecular imperfect symmetry. For MO's, we may use the square of LCAO coefficients to construct the atomic criterion, but owing to the restriction of some molecular symmetry, some of the atomic criteria in some special symmetric positions are always equal. For example, CHX=C=CHX with the same halogens in the process along *cis*-IRC, where the $\mathbf{C}_2$ symmetry will present, the corresponding atomic criteria in relation to X(5) and X(7), H(4) and H(6), or C(2) and C(3) would be always the same, respectively. According to the transformation in $G'_{\mathrm{TS}} = \left\{\hat{M}_{XZ}, \hat{M}_{YZ}\right\}$, the GJ and $G^{\#}J$ are different, but corresponding atomic criteria would be still equality. If the spatial factor is ignored, the membership functions of MO's will always be one. Therefore, the spatial factor should be considered, for such case.

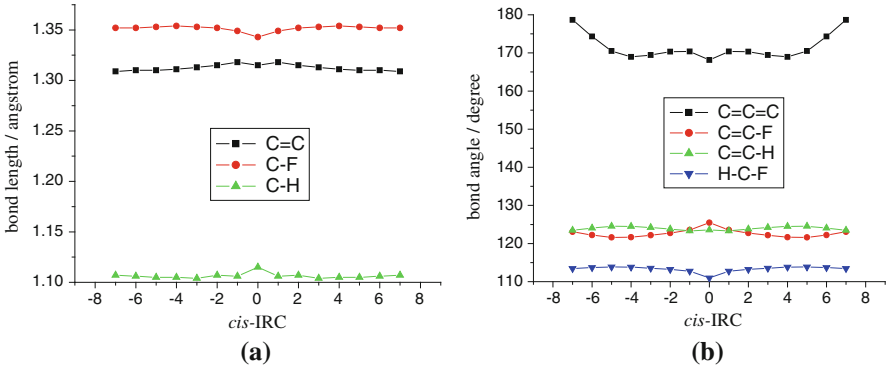


**Fig. 4** The bond length and bond angle of allene-1,3-difluoride (CHF=C=CHF) (vs.) *cis*-IRC through the internal rotation process . **a** Bond length (vs.) *cis*-IRC, **b** bond angle (vs.) *cis*-IRC

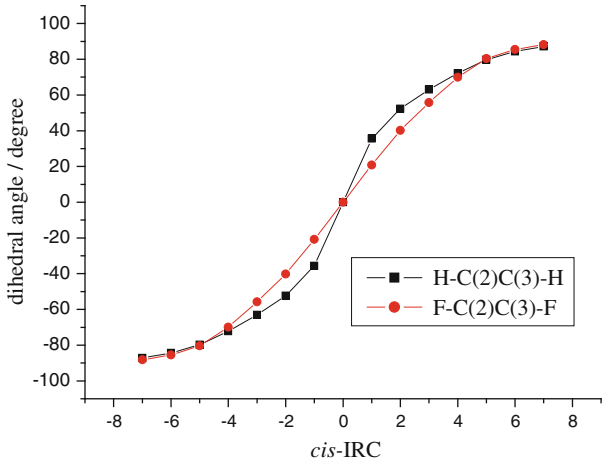


**Fig. 5** The dihedral angle of allene-1,3-difluoride (CHF=C=CHF) (vs.) *cis*-IRC through the internal rotation process (at AM1 level)

To examine the space factor, we study the configuration variation of CHF=C=CHF through the internal rotation process along the *cis*-IRC. Using Gaussian program[22], we may calculate the molecular skeleton configuration along the *cis*-IRC point-by-point and transform to the Cartesian coordinate system chosen above from the output standard orientation. We can then obtain the values of bond lengths and angles of the molecule along the *cis*-IRC as shown in Fig. 4. It can be seen from this figure that the variation is not very significant. The significant variations appear near the *cis*-TS. Along the *cis*-IRC process, dihedral angles, HCCH and FCCF, change significantly, as shown in Fig. 5. For a whole internal rotation process of the molecular chiral transition, the dihedral angle will change up to 180°. In general, in a unimolecular dynamic system without bond formation and breaking, the variation of bond length will be small, but in this case, the effect of the spatial factor on the dihedral angle is large.

As the difference between the positions of GJ atom and $G^{\#}J$ atom is neglected, the membership function of molecule **M** in relation to the symmetric transformation $\left(\hat{G}\right)$, [12–19] $\left(\mu(\hat{G}/\mathbf{M})\right)$ may be defined as:

$$\mu\left(\hat{G}/\mathbf{M}\right) = \left[\sum_{J}\left(Y_J \wedge Y_{GJ}\right)\right] \Big/ \left[\sum_{J}\left(Y_J\right)\right] \tag{2a}$$

As for MO $\Psi_\rho$, the corresponding membership function is:

$$\begin{aligned}\mu\left(\hat{G}/\Psi_\rho\right) &= \left[\sum_{J}\sum_{i}\left(Y_{Ji} \wedge Y_{GJi}\right)\right] \Big/ \left[\sum_{J}\sum_{i}\left(Y_{Ji}\right)\right] \\ &= \sum_{J}\sum_{i}\left[\left(a^*_\rho(J,i)\, a_\rho(J,i)\right) \wedge \left(a^*_\rho(GJ,i)\ a_\rho(GJ,i)\right)\right] \Big/ \\ &\quad \sum_{J}\sum_{i}\left[a^2_\rho(J,i) \wedge a^2_\rho(GJ,i)\right]\end{aligned} \tag{2b}$$

where $Y_{Ji}$ denotes the criterion of the $i$-AO in J-atom, equal to the squire of corresponding LCAO-MO coefficient. For stable molecules, these equations may be used immediately, but for the dynamic process with the significant spatial variation, they will be modified slightly [19]:

$$\mu_E(\hat{G}/\mathbf{M}) = \left[\sum_{J}\left(Y_J \wedge Y_{GJ}\right)\varphi\left(GJ, G^{\#}J\right) / \sum_{J}\sum_{i}\left(Y_{Ji}\right)\right] \tag{3a}$$

$$\begin{aligned}\mu_E\left(\hat{G}/\Psi_\rho\right) &= \left[\sum_{J}\sum_{i}\left(Y_{Ji} \wedge Y_{GJi}\right)\varphi\left(GJ, G^{\#}J\right)\right] \Big/ \left[\sum_{J}\sum_{i}\left(Y_{Ji}\right)\right] \\ &= \sum_{J}\sum_{i}\left[\left(a^*_\rho(J,i)\ a_\rho(J,i)\right) \wedge \left(a^*_\rho(GJ,i)\ a_\rho(GJ,i)\right)\right] \\ &\quad \left[\varphi\left(GJ, G^{\#}J\right)\right] \\ &\quad \Big/ \sum_{J}\sum_{i}\left[a^2_\rho(J,i) \wedge a^2_\rho(GJ,i)\right]\end{aligned} \tag{3b}$$

where $\varphi\left(GJ, G^{\#}J\right)$ may be called space factor, and other terms in relation to $\left(Y_J \wedge Y_{GJ}\right)$ relating to the intrinsic chemical property may be called intrinsic factor. The space factor $\varphi\left(GJ, G^{\#}J\right)$ should be a function of geometric difference between $G^{\#}J$-atom and GJ-atom. Where $G^{\#}J$-atom is the J-atom in the theoretic ideal position after the operation of the well-defined symmetric transformation $\left(\hat{G}\right)$, and GJ-atom is J-atom in the actual position near that of $G^{\#}J$-atom after the operation of the well-defined symmetric transformation. When the positions of GJ and $G^{\#}J$ coincide, $\varphi(GJ,G^{\#}J)$

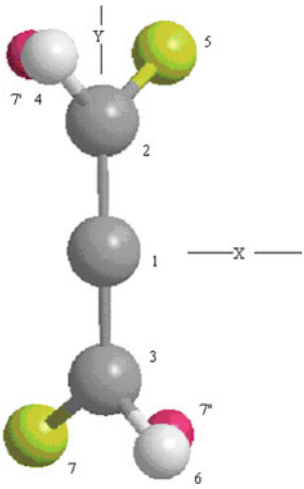


**Fig. 6** The model of CHF=C=CHF through the internal rotation along *cis*-IRC path (for the fuzzy subset symmetry analysis). The image atoms (atomic numbering 7′ and 7″) denoted with the *red balls*. (Color figure online)

Requals one. As GJ and $G^{\#}J$ are very close, Eq. (3b) may be used as a good approximation. Therefore, the membership function of a molecular system with well-defined symmetry in relation to transformation $\hat{G}$ equals one, that is, the criteria of GJ- and J-atoms are equal ($Y_{GJ} = Y_J$) and the space factor $\varphi\left(GJ, G^{\#}J\right) = 1$ (i.e. GJ and $G^{\#}J$ coincide). The positions of GJ and $G^{\#}J$-atoms in a molecule may also be described by the Z-matrix (internal) coordinate system. Since the variation of bond lengths of allene-1,3-dihalides is small during the internal rotation, we will not analyze them. However, because the angle and dihedral angle (especially) are periodic quantities, the relative effect on space factor may be not neglected.

For the internal-rotation of CHF=C=CHF through the *cis*-IRC path, the space factor $\varphi(GJ,G^{\#}J)$ of a carbon atom (J is a carbon atom) is unity. If J is a hydrogen or fluorine atom in the CHF-group, in relation to transformation $\hat{G} = \hat{E}$ or $\hat{C}_2$, GJ and $G^{\#}J$ will also coincide, and so $\varphi(GJ,G^{\#}J)$ equals unity; but, in relation to transformation $\hat{G} = \hat{M}_{XZ}$ or $\hat{M}_{YZ}$, GJ and $G^{\#}J$ may be not coincide, the difference would depend on the dihedral angle, HCCH($\theta_{DH}$) or FCCF($\theta_{DF}$), as shown in Fig. 5. Similar as allene [19], we may have:

$$\varphi\left(GJ,\ G^{\#}J\right) = \mathrm{abs}(\cos(\theta D)) \tag{4}$$

where $\theta_D$ may be $\theta_{DH}$ or $\theta_{DF}$.

We first consider J-atom as F(7) in relation to transformation $\hat{G} = \hat{M}_{XZ}$ or $\hat{M}_{YZ}$, as shown in Fig. 6 . The image atoms, 7′ and 7″, denote $G^{\#}J$-atoms corresponding to $\hat{G} = \hat{M}_{XZ}$ and $\hat{M}_{YZ}$ on J-atoms, F(5) and F(7), respectively. $\theta_{DF}$ in Eq. (4) is the dihedral angle between plane (7′)C(2)C(3) and F(5)C(2)C(3) or between plane (7″)C(3)C(2) and F(7)C(3)C(2). Similar analysis may also be done for the $\theta_{DH}$ easily, but it is omitted here.

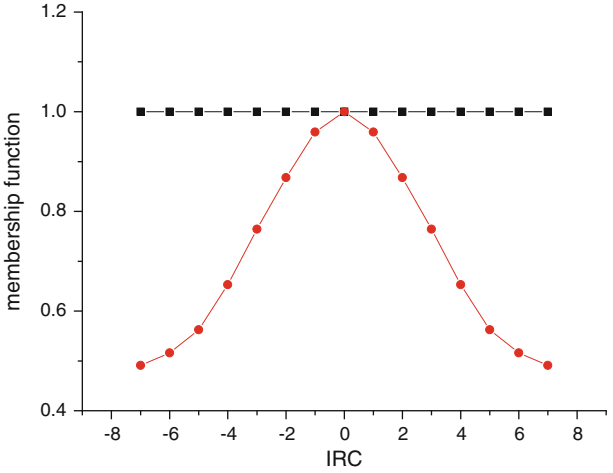


**Fig. 7** The membership function of CHF=C=CHF molecular skeleton (vs.) *cis*-IRC (through the internal rotation *cis*-IRC path, at AM1 level). *Black line* for $\hat{C}_2$, $\hat{R}\hat{M}_{XZ}$ or $\hat{R}\hat{M}_{YZ}$; *red curve* for $\hat{R}\hat{R}$, $\hat{M}_{XZ}$ or $\hat{M}_{YZ}$. (Color figure online)

If GJ- and $G^{\#}$J-atoms coincide, such as, if J-atom equals to F(7) or F(5), the membership function $\left(\mu\left(\hat{G}/\mathbf{M}\right)\right)$ in relation to $\hat{E}$, $\hat{C}_2$, $\hat{R}\hat{M}_{XZ}$ and $\hat{R}\hat{M}_{XZ}$ will equal to one. Here the $\theta_D$ is the dihedral angle between the plane GJ-C(2)C(3) and $G^{\#}$J-C(2)C(3). According to Eq. (4), if $\theta_D$ is 0° (i.e. TS), and GJ- and $G^{\#}$J-atoms coincide, so $\varphi$(GJ,$G^{\#}$J) is 1; yet if $\theta_D$ is 90°, and GJ- and $G^{\#}$J-atoms are separated maximally, $\varphi$(GJ,$G^{\#}$J) is 0. This indicates that Eq. (4) is reasonable. As mentioned above, for CHF=C=CHF molecular skeleton, we may obtain its membership function variation in relation to some symmetric transformation through the *cis*-IRC path, as shown in Fig. 7.

Since this system has well-defined symmetry in relation to $\hat{C}_2$, $\hat{R}\hat{M}_{XZ}$ and $\hat{R}\hat{M}_{YZ}$, corresponding $\mu(\hat{G}/\mathbf{M})$ always equals to one, and corresponding space factors, $\varphi$(GJ, $G^{\#}$J), equal one, too. However, in relation to transformations $\hat{R}\hat{M}_{XZ}$ and $\hat{M}_{YZ}$, only TS have well-defined symmetry. It means that $\mu(\hat{G}/\mathbf{M})$ will be equal to one only in the case of IRC equal to 0, i.e. the TS. But $\mu(\hat{G}/\mathbf{M})$ would be less than one as it is not TS, and it will change with the variation of IRC. According to the IRC-scale, $\mu(\hat{G}/\mathbf{M})$ (vs.) IRC curve will be symmetric about TS (IRC=0).

It is notable that for the molecule skeleton the atomic criterion $Y_J$ should be invariant and determined by the intrinsic property of the atom itself. For CHF=C=CHF, the wrong inference of $Y_J = Y_{GJ}$ will follow if we assume all space factors equal to one. The cause of the membership function less than one is thus introduced by the space factor rather than by the intrinsic factor.

Since the membership functions of a well-defined symmetry system equal to one [13], the corresponding symmetric element will be determined in only one way. For example, the *cis*-TS belongs to the well-defined $C_{2V}$ group, so all the elements in $C_{2V}$ will be chosen in only one way. However, for the approximate symmetry system, the related symmetric elements may be chosen in many ways. In the case of the *cis*-IRC

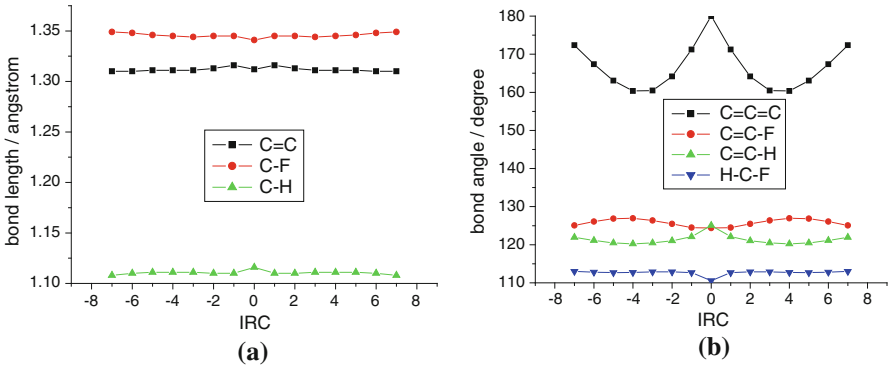


**Fig. 8** The bond length and bond angle of allene-1,3-difluoride (CHF=C=CHF) (vs.) *trans*-IRC through the internal rotation process. **a** Bond length (vs.) *trans*-IRC, **b** bond angle (vs.) *trans*-IRC

states other than the TS, although the well-defined $\mathbf{C}_2$ axis is chosen in only way, the pair of mirrors, which are perpendicular to each other and cross in the $\mathbf{C}_2$ axis, may be chosen in various ways as long as they conform to the way for choosing the TS symmetric elements. Because the all states in this IRC path have well-defined symmetry $C_2$, the relative space factor should be always one. According to Cartesian coordinate system for analyses the approximate symmetry, we must modify the setting of the standard orientation of the Gaussian program. We choose the $C_2$ axis in $C_{2V}$ point group as $Z$-axis, and the two orthogonal mirror planes in the group as XZ- and YZ-planes. There are various ways to choose the origin, such as at C(1) atom centre or at the midpoint of the line connecting C(2) and C(3). For the *cis*-IRC process, both ways of choosing origin are allowed and could be used to analyze the approximate symmetry. In the states other than TS, the mirror planes in $C_{2V}$ will be changed to each other, the $\mu\left(\hat{G}/\mathbf{M}\right)$ values will be less than one. Whatever the origin is chosen, the geometry of corresponding mirror planes should be the same. Therefore, even the membership functions of molecular skeleton and MO's would be less one, but they will not change with the variation of the origin choice.

States along the *trans*-IRC path may be analyzed similarly. The relationship of bond length and bond angle in 1,3-difluoride-allene molecule (vs.) *trans*-IRC are shown in Fig. 8. It can be seen that through the internal rotation *trans*-IRC process, the bond length changes only in a small amount, but the bond angle changes more obviously than that through the *cis*-IRC process, e.g., more than 20° variation in angle C=C=C.

During the IRC processes, though the two TS's (*cis*-TS and *trans*-TS) are planar molecules, their symmetries are different. As shown in Fig. 1, the *cis*-TS and *trans*-TS belong to $C_{2V}$ and $C_{2h}$ group, respectively. Particularly, the $C_2$ axis remains in the whole internal rotation process, and it lies either on the molecular plane of the *cis*-TS or vertical to the molecular plane of the *trans*-TS. Through the *cis*-IRC process, backbone C=C=C maintains $C_{2V}$ symmetry to which *cis*-TS belongs, only the hydrogen and fluorine atoms deviate from the TS molecular plane. However, through the *trans*-IRC process, C=C=C cannot maintain $C_{2h}$ symmetry to which the *trans*-TS belongs. Therefore, when we analyze the approximate symmetry in relation to the

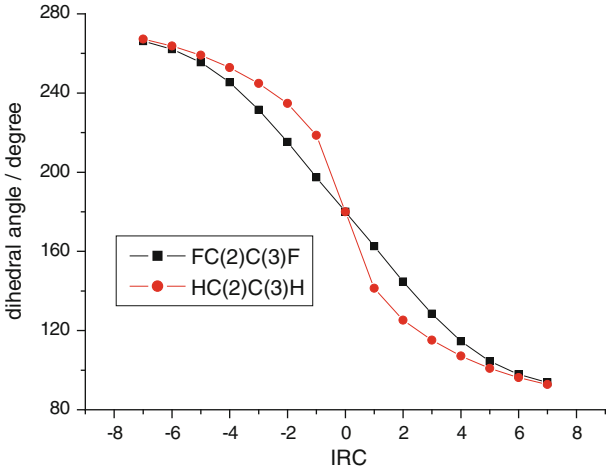


**Fig. 9** The dihedral angle of allene-1,3-difluoride (CHF=C=CHF) (vs.) *trans*-IRC through the internal rotation process (at AM1 level)

transformations in $C_{2h}$, we should consider the space factor not only of hydrogen and fluorine but also of carbon atoms.

Some dihedral angles will change more obviously in the *trans*-IRC process, as shown in Fig. 9. To combine with Fig. 5, we thus cover both processes along *cis*-IRC and *trans*-IRC. However, the initial and final states through the *trans*-IRC process are chosen as the final and initial states through the *cis*-IRC process, respectively, although we may choose them the other way around and obtain essentially the same results.

The symmetric transformations including in the point groups to which *trans*-TS ($C_{2h}$) and *trans*-IRC states other than TS ($C_2$) belong are:

$$\begin{aligned} C_{2h} : G_{trans-TS} &= G_{trans-IRC} \cup G'_{trans-TS} = \left\{\hat{E}, \hat{C}_2\right\} \cup \left\{\hat{P}, \hat{M}_h\right\} \\ &= \left\{\hat{E}, \hat{C}_2, \hat{P}, \hat{M}_h\right\} \end{aligned} \tag{5a}$$

$$C2 : G_{trans-IRC} = \left\{\hat{E}, \hat{C}_2\right\} \tag{5b}$$

where $\hat{P}$ is the space inversion with C(1) as inversion centre, and $\hat{M}_h$ is the reflection about the XY reflection plane. Through the whole *trans*-IRC process, all states have the $C_2$ symmetry, but the *trans*-TS has an extra symmetry included in the $G'_{trans-TS} = \left\{\hat{P}, \hat{M}_h\right\}$ set whereas other states have only the approximate symmetry related to $G'_{trans-TS}$. In additional, they have the symmetry related to the joint transformations $\hat{R}\hat{P}$ and $\hat{R}\hat{M}_h$. Consequently, $\mu\left(\hat{G}/\mathbf{M}\right)$ of all states through the *trans*-IRC related to operation $\hat{E}$, $\hat{C}_2$, $\hat{R}\hat{P}$ and $\hat{R}\hat{M}_h$ equal to one. The symmetric element in connection with the approximate symmetry may be chosen in different ways with different corresponding $\mu\left(\hat{G}/\mathbf{M}\right)$ as mentioned above. Firstly, for the molecule with $C_{2h}$ symmetry, in

the standard orientation, the Gaussian program chooses $C_2$ as the $Z$-axis, and the two orthogonal reflection planes as the XZ- and YZ-coordinate planes. Secondly, the origin of the Cartesian coordinate system may be chosen on C(1), and the plane through the origin but perpendicular to $Z$-axis may be chosen as the Cartesian coordinate XY-plane ( i.e. the molecule plane of *trans*-TS). Thirdly, as C=C=C is not a straight line through the *trans*-IRC, we may also choose line connecting C(2)C(3) as the $Y$-axis, then the corresponding YZ- and XZ-coordinate planes are obtained readily with the origin at C(1) or the midpoint of C(2)C(3). As mentioned above, for the *trans*-TS, the Cartesian coordinate system is definite, but the states through the *trans*-IRC, deviating from the TS, the molecular symmetry will decrease from $C_{2h}$ to $C_2$, with only the less membership function in relation to $\hat{P}$ and $\hat{M}_h$ [14–17]. When we take the first Cartesian coordinate system for the whole *trans*-IRC states, for the different origin options, the $\mu\left(\hat{G}/\mathbf{M}\right)$ values for $\hat{P}$ and $\hat{M}_h$ will be different except for the *trans*-TS.

In the choice with the origin and space inversion centre chosen on the midpoint of line C(2)C(3), the operations for $\hat{G} = \hat{P}$ and $\hat{M}_h$ will swap the positions of J-atom C(2) and C(3), and GJ equals $G^{\#}J$ as well as atom criteria $Y_J$ equals $Y_{GJ}$, and the space factor $\varphi(GJ,G^{\#}J)$ equals 1. However, the above same operations will change the position of J-atom C(1) to an image $G^{\#}J$-atom. As GJ is not equal to $G^{\#}J$, the space factor $\varphi(GJ,G^{\#}J)$ will be less than 1. Similar to Eq. (4), we define the space factor:

$$\varphi\left(GJ, G^{\#}J\right) = \text{abs}(\cos(\theta_C)) \tag{6}$$

Here $\theta_C = \angle\left(GJ, AX, G^{\#}J\right)$ and AX may be C(2) or C(3). If C=C=C is in a straight line, $\theta_C = 0$ and space factor $\varphi(GJ,G^{\#}J) = 1$. If J-atom is H or F atom, we may analyze the approximate symmetry similarly as the *cis*-IRC state. Of course, it should be noted that for a certain J-atom, corresponding $G^{\#}J$ image-atom and real GJ-atom for $\hat{P}$, $\hat{M}_h$, $\hat{M}_{XZ}$ and $\hat{M}_{YZ}$ are different.

Once the Cartesian coordinate system is defined, $\varphi(GJ,G^{\#}J)$ and $\mu\left(\hat{G}/\mathbf{M}\right)$ of each atom may be obtained. For CHF=C=CHF molecular skeleton, the relationship between the membership function (vs.) *trans*-IRC is shown in Fig. 10. These results seem to be similar to those of *cis*-IRC path (Fig. 7), but they are in fact different. The internal-coordinate configuration with the same IRC-value along the *trans*-IRC is different from that along the *cis*-IRC. For the *trans*-IRC path, the red curve shown in Fig. 10 denote $\mu\left(\hat{G}/\mathbf{M}\right)$ with $\hat{G}$ of $\hat{M}_h$ or $\hat{P}$, but for the *cis*-IRC path, the red curve shown in Fig. 7 denote $\mu\left(\hat{G}/\mathbf{M}\right)$ with $\hat{G}$ of $\hat{M}_{XZ}$ or $\hat{M}_{YZ}$. Taking C(1) atom as the space inversion centre and the origin, we may analyzed them similarly except for the TS, and found that $\mu\left(\hat{G}/\mathbf{M}\right)$ values are somewhat smaller as the green curve shows in Fig. 10.

Sometimes, the space factor will be important for the approximate symmetry, but the intrinsic factor is often more important in the chemistry process. Meanwhile the MO membership function controlled by the space factor could not be attributed to the overlap of various irreducible representations. For example, the spectra selection rule of molecules depends mainly on the intrinsic factor.

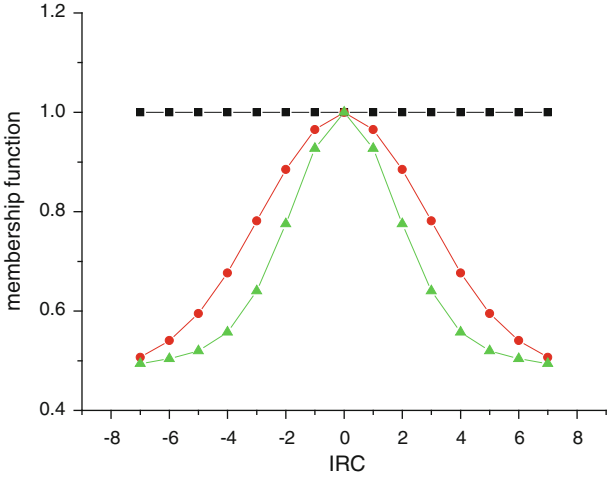


**Fig. 10** The membership function of CHF=C=CHF molecular skeleton (vs.) *trans*-IRC through the internal rotation *trans*-IRC path (at AM1 level). *Black line* for $\hat{C}_2$, $\hat{R}\hat{M}_h$ or $\hat{R}\hat{P}$; *red curve*: origin set at the midpoint of C(2)C(3), for $\hat{R}$, $\hat{M}_h$ or $\hat{P}$; *green curve*: origin set at C(1), for $\hat{R}$,$\hat{M}_h$ or $\hat{P}$. (Color figure online)

By the way, it may be shown that where an approximate symmetry system may be in relation to the membership function with the less value (not near one), i.e. not the approximate (perfect) symmetry.

## 2.3 Membership function and irreducible representation component

The MO imperfect symmetry is related to two important parameters: membership function and irreducible representation component. We first calculated a few IRC-value configurations for allene-1,3-dihalides at AM1 level, and then we used the linear interpolation to obtain the configuration pairs with opposite IRC values. After that, we calculated the single-point energies for these configurations at the same level. For this system, we examined 22 MO's which were combined by valence AO's of the three carbon, two halogen and two hydrogen atoms. At AM1 level [22], we have 14 occupied MO's (OMO) and 8 virtual MO's (VMO). With the single-point results through the IRC path, the membership functions and the irreducible representation components of each MO may be obtained. In the calculation of the irreducible representation component, the standard orientation in from the Gaussian calculation needs to transform to the coordinate system mentioned in Sect. 2.1.

For allene-1,3-dihalides with different halogen atoms, there is no complete $C_2$symmetry, but only related fuzzy subset:

$$\underset{\sim 2}{C} = \left(1/\hat{E}\right) + \left(\mu/\hat{C}_2\right) \tag{7}$$

where $\hat{E}$ denotes the identity, and $\mu$ the membership function related to $\hat{C}_2$ transformation. The fuzzy representation which MO belongs to is an overlap of two pure representations A, symmetric, and B, anti-symmetric,

$$\underset{\sim}{\Gamma} = \text{Xg A} + \text{Xu B} \tag{8}$$

where Xg and Xu are the pure symmetric and pure anti-symmetric representation components, respectively.

According to the conservation rule of the molecule orbital (W-H rule), both symmetry and invariant are important [25]. They are different concepts [23,24]. Viewed from the chemical symmetric theory, they may denote either the point group to which the molecular skeleton belongs and the irreducible representation to which the MO belongs, respectively. In essence, the W-H rule means that as the molecular skeleton can always maintain the symmetry in relation to a certain group, then the MO's of corresponding molecule would be unchanged under the irreducible representations of such group. As to the fuzzy subset theory of approximate symmetry, we need to examine the fuzzy subset (especially the membership function of subset element) and the fuzzy representation (especially the representation component). For this molecular system, Eqs. (7) and (8) are related to the above concepts. To understand their relationship, we consider the simplest model, a diatomic molecular AB, and suppose that the MO ($\psi$) is combined by two AO's ($\phi_{\mathrm{A}}$ and $\phi_{\mathrm{B}}$), one from each atom, i.e.

$$\psi = a_{\mathrm{A}}\phi_{\mathrm{A}} + a_{\mathrm{B}}\phi_{\mathrm{B}} = \left(a_g + a_u\right)\phi_{\mathrm{A}} + \left(a_g - a_u\right)\phi_{\mathrm{B}} \tag{9}$$

where $a_{\mathrm{A}}$ and $a_{\mathrm{B}}$ are the normalized LCAO-MO ($\psi$) coefficients of $\phi_{\mathrm{A}}$ and $\phi_{\mathrm{B}}$, respectively. Set $a_{\mathrm{A}}^2 > a_{\mathrm{B}}^2$ and $a_{\mathrm{A}} > 0$, these coefficients may be decomposed to two parts: the symmetric part $a_g$ and the anti-symmetric part $a_u$, according to a certain $C_2$ axis symmetric transformation. From Eq. (9), we have:

$$a_g = \left(a_{\mathrm{A}} + a_{\mathrm{B}}\right)/2 \tag{10a}$$

$$a_u = \left(a_{\mathrm{A}} - a_{\mathrm{B}}\right)/2 \tag{10b}$$

According to the definition of the membership function [7–9] for MO $\psi$ under the symmetric transformation $\hat{\mathrm{G}}$, we have,

$$\mu = \left(a_{\mathrm{A}}^2 \wedge a_{\mathrm{B}}^2\right) + \left(a_{\mathrm{B}}^2 \wedge a_{\mathrm{A}}^2\right) = 2\,a_{\mathrm{B}}^2 \tag{11}$$

Meanwhile for transformation $\hat{\mathrm{G}}$, the symmetric and anti-symmetric components are:

$$\mathrm{Xg} = 2\,a_g^2 \quad \& \quad \mathrm{Xu} = 2\,a_u^2 \tag{12}$$

For a certain $\mu$ value, from the Eq. (11), we can obtain a pair of $a_{\mathrm{B}}$, i.e. $a_{\mathrm{B}} = \pm(\mu/2)^{0.5}$. Using the MO normalized condition and Eq. (12), we may find $a_{\mathrm{A}}$ (>0) and Xg and Xu. Since a certain $\mu$ value, $a_{\mathrm{B}}$ has two values, the solution of Xg (or Xu) should also have two values. Therefore, for the simplest model, we obtain the relationship diagram of $\mu$(vs.) Xg as shown in Fig. 11, where the black curve responds to the Xg > 0.5, indicating main symmetric representation, whereas the red curve responds to Xg < 0.5, indicating main anti-symmetric representation. When Xg equals 0.5, the membership

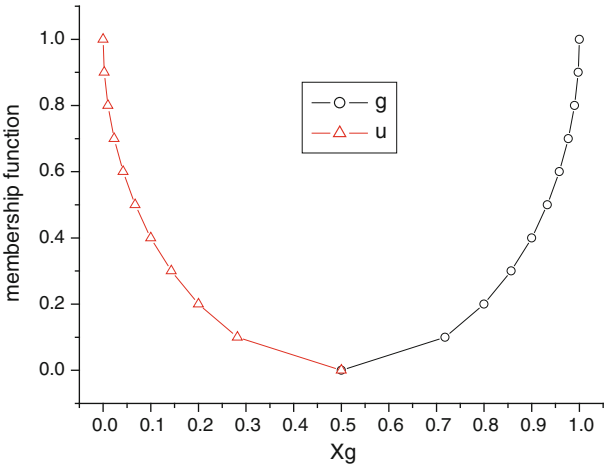


**Fig. 11** The membership function (vs.) symmetric representation component diagram for $\hat{C}_2$ transformation for the simplest MO model

function equals zero, and $a_g$ equals $a_u$, $a_B$ equals 0, and $a_A$ equals 1. In such case, the MO is only the AO $\phi_A$. When Xg equals 0 (pure anti-symmetric representation) or 1 (pure symmetric representation), the membership function will be one. As shown in Fig. 11, when the MO approaches to pure representation, the small change of the representation component may cause the large variation of the membership function. However, when the symmetry is poor, the membership function will change slightly. For more complex MO, the relationship between the membership function (vs.) representation component will be also more complex, while the curve in Fig. 11 will the boundary.

## 3 Approximate symmetry characteristics of CHF=C=CHF

For allene-1,3-dihalides with the same halogen atoms, CHF=C=CHF will be taken as a prototype. For this molecule may internally rotate through the *cis*-IRC or the *trans*-IRC path. The related TS, shown in Fig. 1, are plane molecules with $C_{2v}$ and $C_{2h}$ point group symmetry, respectively. Through the internal rotation process, the molecule will be undergoing the chiral transition. The variation of molecular potential energy (vs.) IRC is shown in Fig. 12. The maxima of the energy curves are TS's, and both curves are the symmetrically distributed about the TS's.

Through a certain IRC path (*cis*- or *trans*-), as molecular system may always maintain a well-defined symmetry in relation to $G_{IRC}$ point group, so related membership functions of such molecular system should be always one in relation to the all symmetric transformation included by $G_{IRC}$ point group. In addition, the TS may maintain the well-defined symmetry in relation to $G_{TS}$ point group:

$$G_{TS} = G_{IRC} \cup G'_{TS} \tag{13}$$

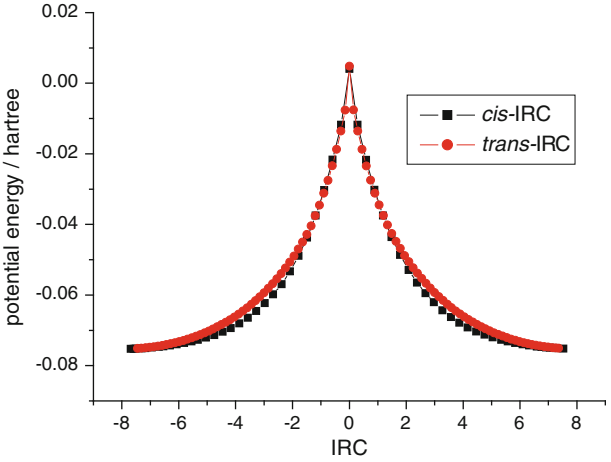


**Fig. 12** The molecular potential energy (at AM1 level) through the internal rotation of CHF=C=CHF. *Black line* for the *cis*-IRC; *red line* for the *trans*-IRC. (Color figure online)

Here $G'_{TS}$ denotes the symmetric transformation set which include in TS, but not in the IRC states other than TS. For TS, the membership functions in relation to the $\hat{R}$ would be equal one, but less one for the state other than TS, which may often be the same as that in relation to the transformations in $G'_{TS}$ set.

### 3.1 Approximate symmetry characteristic for the *cis*-IRC path

From Gaussian [22], 22 valence shell MO's of CHF=C=CHF are obtained at AM1 level. The calculated variation of MO-energy in connection with relative 22 MO's (14 OMO's and 8 VMO's) (vs.) *cis*-IRC path is shown in Fig. 13, where (A): for the all 22 MO's (B): for the near frontier MO's. In this Figure, OMO1 and VMO1 denote the HOMO and LUMO, respectively, and other suffixes denote the order starting from the two frontier MO's. It is shown that through the IRC the MO energy correlation lines have $C_2$ group symmetry. Corresponding to the case of cross lines, there are two times through the whole process from reactant to product.

The irreducible representations of $C_{2V}$ group that the *cis*-TS belongs to are $A_1$, $A_2$, $B_1$ and $B_2$, to one of which the MO's must belong. Here A and B denote $C_2$ symmetric and anti-symmetric rotation transformations, respectively, while subscripts 1 and 2 denote symmetric or anti-symmetric reflection transformations. Since there is no well-defined symmetry for the IRC states other than TS, so in the correlation diagram, there is no need to consider the irreducible representation. We may still analyze their fuzzy symmetry. On the other hand, there is well-defined symmetry in relation to the joint transformations of the reaction reversal $\hat{R}_c$ and the above two mirror reflections ($\hat{M}_{XZ}$ and $\hat{M}_{YZ}$) $\hat{R}_C\hat{M}_{XZ}$ and $\hat{R}_C\hat{M}_{YZ}$, where $\hat{R}_C$ denotes the reaction reversal transformation according to the *cis*-IRC in the chiral transition process. Therefore, all *cis*-IRC states belong to well-defined symmetry in relation to group $G(RM)_C$ defined below,

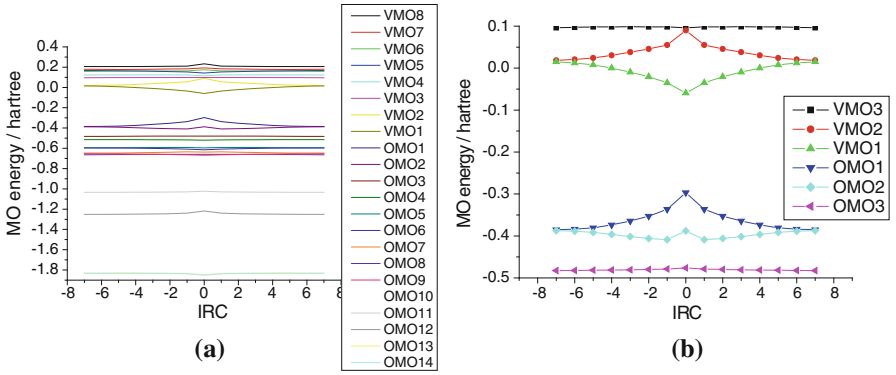


**Fig. 13** The CHF=C=CHF MO energy variation diagram through the internal rotation *cis*-IRC path at AM1 level. **a** For all MO's, **b** near frontier MO's

**Table 1** Irreducible representations and characters of $G(R_cC_{2v})$ transformation group

| | $\hat{E}$ | $\hat{C}_{2Z}$ | $\hat{R}_c\hat{M}_{XZ}$ | $\hat{R}_c\hat{M}_{YZ}$ |
|---|---|---|---|---|
| $rA_1$ | 1 | 1 | 1 | 1 |
| $rA_2$ | 1 | 1 | −1 | −1 |
| $rB_1$ | 1 | −1 | 1 | −1 |
| $rB_2$ | 1 | −1 | −1 | 1 |

$$G(RM)_C \equiv G(R_cC_{2v}) = \left\{\hat{E}, \hat{C}_2, \hat{R}_C\hat{M}_{XZ}, \hat{R}_C\hat{M}_{YZ}\right\} \tag{14}$$

whose characters are shown in Table 1.

The symmetry of group $G(R_cC_{2v})$ will remain in the whole internal rotation *cis*-IRC path of CHF=C=CHF. For TS, reaction reversal $\hat{R}_C$ is equivalent to $\hat{E}$, and so irreducible representations and characters in Table 1 will be reduced to those of $C_{2v}$ group (and "r" will be omitted). Through the whole *cis*-IRC path, the membership functions of the molecule skeleton and of all the MO's in relation to four symmetric transformations should be one; all the MO's are the common eigenstates of the transformations. The eigenvalue (axis parity) of MO under $\hat{C}_2$ operation may be determined as in a point group, and it is either 1 (symmetric) or -1 (anti-symmetric). Since for the *cis*-TS, $\hat{R}_C$ and $\hat{E}$ are equivalent, and so the eigenvalues in relation to joint transformation $\hat{R}_C\hat{M}_{XZ}$ and $\hat{R}_C\hat{M}_{YZ}$ may be determined by means of those in relation to $\hat{M}_{XZ}$ and $\hat{M}_{YZ}$ at relative TS.

However, the single transformations in the *cis*-IRC states other than *cis*-TS, $\hat{R}_C$, $\hat{M}_{XZ}$ and $\hat{M}_{YZ}$, are not well-defined. All of the calculated membership functions of MO's using Eqs. (3) and (4) are less than one. As shown in Fig. 14, straight line MFC indicates that all MO membership functions related to transformations $\hat{C}_2$, $\hat{R}_C\hat{M}_{XZ}$ and $\hat{R}_C\hat{M}_{YZ}$ equal one, but the curves show the variation of the related MO membership functions in relation to the $\hat{M}_{XZ}$ and $\hat{M}_{YZ}$ (vs.) IRC. All of these curves appear symmetric about TS, and reach maxima at the same point. This variation stems from the space factor, $\varphi(GJ,G^{\#}J)$, which is less than one. If the symmetry condition in relation

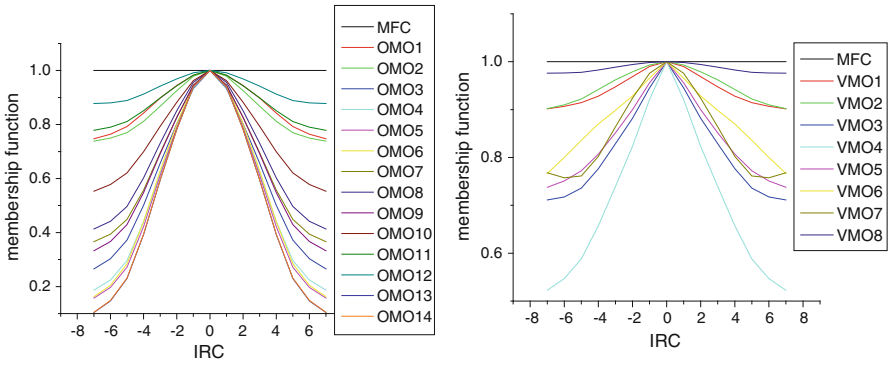


**(a)** OMO's **(b)** VMO's

**Fig. 14** The membership function of CHF=C=CHF MO's (vs.) IRC through the internal rotation *cis*-IRC path at AM1 level

to $\hat{G} = \hat{C}_2$, $Y_J = \left[a^*_\rho (J, i)\, a_\rho (J, i)\right]$ and $Y_{GJ} = \left[a^*_\rho (GJ, i)\ a_\rho (GJ, i)\right]$,were set, that is, the space factor were set to one, all the membership functions would be incorrectly set to one. Similar error in the MO membership function will also be introduced by the space factor, but not by the atom criterion. Although the atomic interval, especially the BMO atomic interval, may change the atom criterion, and make the space factor be ignored sometimes, the above effect could not be neglected.

Through the whole *cis*-IRC process, the $G(RC_{2v})$ symmetry maintains, and so the related process is symmetry allowed. In addition, $C_2$ must also be conserved since $C_2$ group is a subgroup of $G(RC_{2v})$.

## 3.2 Approximate symmetry characteristics for the *trans*-IRC path

The AM1 energies of the 22 valance MO's of CHF=C=CHF (vs.) *trans*-IRC are shown in Fig. 15, and the membership functions are shown in Fig. 16. The curves in Fig. 16 are obtained using the irreducible representation of $C_2$ point group which exists in the whole process. As shown by the correlation diagram in Fig. 17, similar to Fig. 13, some twice-cross curves through the internal rotation process *trans*-IRC path are shown. For different choices of Cartesian coordinate system, the LCAO-MO formulae may differ, but the MO energies will be the same. According to W-H rule [23–25], through the internal rotation along the *trans*-IRC path, at TS, CHF=C=CHF will belong to $C_{2h}$ point group, while other states will only belong to a subgroup $C_2$ of $C_{2h}$. $C_2$ has two irreducible representations, A (symmetric) and B (anti-symmetric) under $C_2$ operation, with relative generalized parity (axis parity) of 1 and $-1$, respectively. However, irreducible representations of $C_2$ in $C_{2h}$ group become more complicated, that is, symmetric $A_g$ and $A_u$, and the anti-symmetric $B_g$ and $B_u$. Through the *trans*-IRC process, the reagent and product molecules are a pair of optical enantiomers; and the MO energy (vs.) IRC curves ought to be symmetric about the TS as shown in Fig. 15. The TS should not be optically active. These results are similar to those of the *cis*-IRC, though their point groups differ.

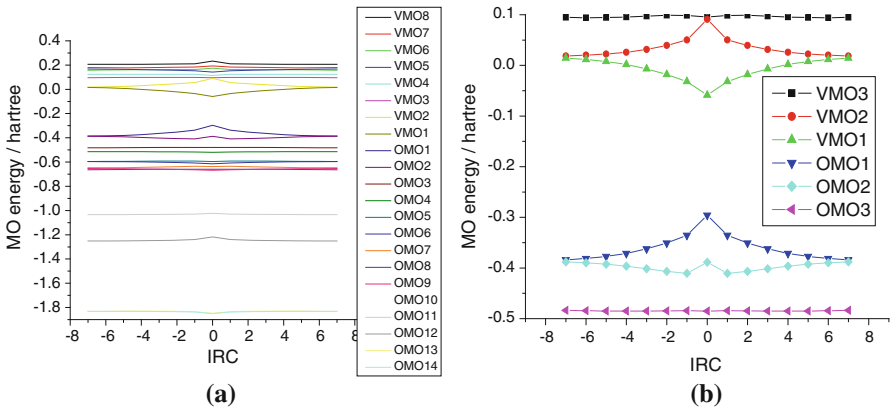


**Fig. 15** The CHF=C=CHF MO energy variation diagram through the internal rotation *trans*-IRC path at AM1 level. **a** For all valance shell MO's, **b** near frontier MO's

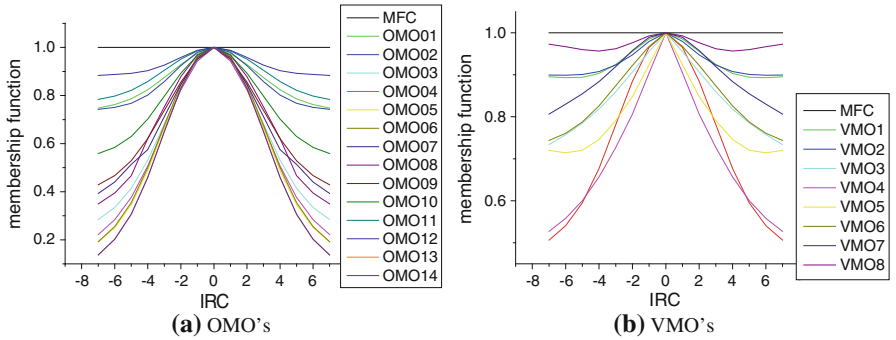


**Fig. 16** The membership function of CHF=C=CHF MO's (vs.) *trans*-IRC path through the internal rotation at AM1 level

Although the *trans*-IRC states other than TS state are not well-defined under $\hat{P}$ and $\hat{M}_{XY}$, they are well-defined under reaction reversal transformations $\hat{R}\hat{P}$ and $\hat{R}\hat{M}_{XY}$. All *trans*-IRC states such as those of CHF=C=CHF belong to group $G(RC_{2h})$ defined below,

$$G(RC_{2h}) == \left\{\hat{E}, \hat{C}_2, \ \hat{R}_t\hat{P}, \ \hat{R}_t\hat{M}_{XY}\right\} \tag{15}$$

The relative irreducible representations and characters are presented in Table 2. At TS, $\hat{R}_t$ will be the same as $\hat{E}$, and this group will reduce to $C_{2h}$ and "r" before the irreducible representations in Table 2 will be dropped.

Through the whole *trans*-IRC, for CHF=C=CHF molecular skeleton and all MO's, their membership functions in relation to all of the symmetric transformation in $G(RC_{2h})$ are equal to one, and so the MO's are the common eigenstates of all the four transformations. The eigenvalue (axis parity) of $\hat{C}_2$ which is 1 (S, symmetric) or $-1$ (A, anti-symmetric), may be obtained as usual. The eigenvalues of the joint

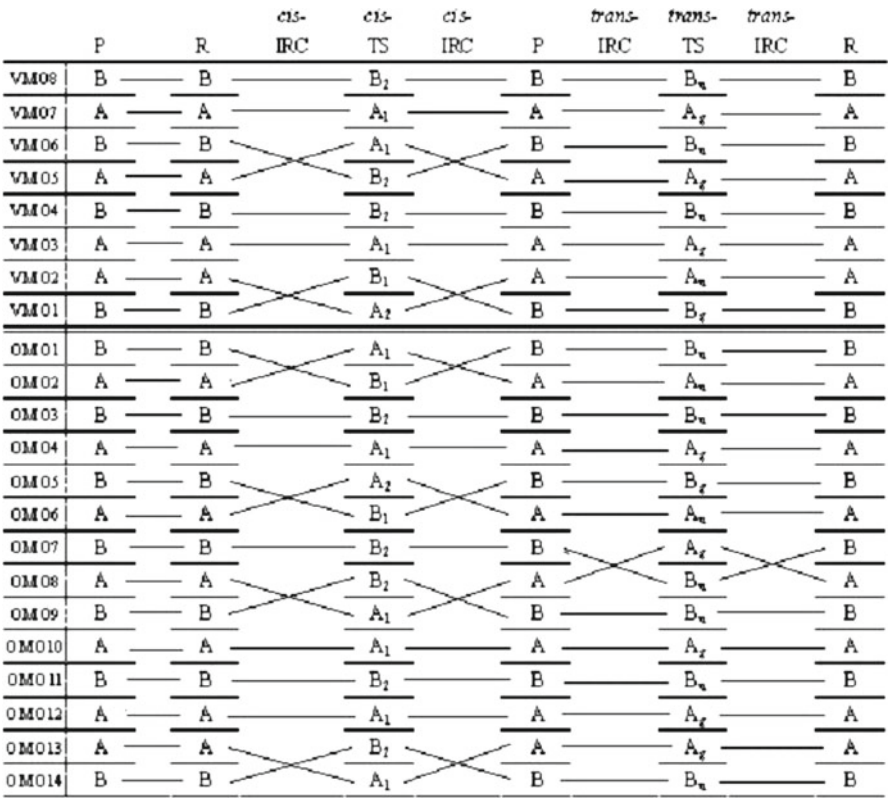


**Fig. 17** $\hat{C}_2$-MO correlation diagram for CHF=C=CHF internal rotation process

**Table 2** Irreducible representations and characters of $G(R_tC_{2h})$ transformation group

| | $\hat{E}$ | $\hat{C}_{2Z}$ | $\hat{R}_t\hat{M}_{XY}$ | $\hat{R}_t\hat{P}$ |
|---|---|---|---|---|
| $rA_g$ | 1 | 1 | 1 | 1 |
| $rA_u$ | 1 | 1 | −1 | −1 |
| $rB_g$ | 1 | −1 | −1 | 1 |
| $rB_u$ | 1 | −1 | 1 | −1 |

transformations, $\hat{R}_t\ \hat{P}$ and $\hat{R}_t\ \hat{M}_{XY}$ may also be 1 (S) or −1 (A), determined by the eigenvalues related to those of $\hat{P}$ and $\hat{M}_{XY}$ of the TS, respectively. As obtained similarly for the *cis*-IRC states, the relative membership functions of the *trans*-IRC states other than TS are less one, which may be affected by a different choosing of Cartesian coordinate system. If we set the space reversal centre and coordinate system origin at C(1), the midpoint of C(2)C(3), the membership functions in relation to $\hat{R}_t$, $\hat{P}$ and $\hat{M}_{XY}$ transformation may be different. However, with well-defined symmetry, $\hat{C}_2$, $\hat{R}_t\hat{M}_{XY}$, $\hat{R}_t\hat{P}$, and related MO's and molecular skeleton, have membership functions of one, not dependent on the way for choosing the space reversal centre and

coordinate system origin. Here we only analyze the case in connection with the centre and origin chosen at the midpoint of C(2)C(3).

Through the *trans*-IRC path, the membership functions in relation to the symmetric transformations $\hat{R}_t$, $\hat{M}_{XY}$ and $\hat{P}$ are the same for the same MO as shown (vs.) IRC in Fig. 16. Similar to the *cis*-IRC case shown in Fig. 14, the membership function reaches the maximum at TS with the value of one, symmetric distributed about TS. Nevertheless, for the same IRC values shown in the two Figures, the relative symmetric transformations and the molecular configurations are different.

Similar to the *cis*-IRC path, through the whole *trans*-IRC path the relative states have $G(RC_{2h})$ symmetry and conserve the related generalized parity (Table 2). For the *trans*-IRC process, space factor $\varphi(GJ,G^{\#}J)$ may also be responsible for the membership function values (less one). Meanwhile, due to symmetric condition, $Y_J = \left[a^*_\rho(J,i)\ a_\rho(J,i)\right]$ and $Y_{GJ} = \left]a^*_\rho(GJ,i)\,a_\rho(GJ,i)\right]$ would be always equal. The space factor makes the MO membership functions decrease directly, not due to the overlap of symmetric and anti-symmetric MO's.

### 3.3 MO correlation diagram for *cis*- and *trans*-IRC internal rotation paths

As mentioned above, through the *cis*- or *trans*-IRC path of CHF=C=CHF, the relative symmetry selection rule depends on the well-defined $C_2$ group. Meanwhile, for all MO's, the irreducible representations may be adapted to make the processes symmetry allowed. Usually, W-H rule is used via the MO correlation diagram based on the symmetry through the whole process. Therefore, we also examined the MO correlation diagram as shown in Fig. 17 in relation to $C_2$ group. This figure shows the MO irreducible representation, where P and R denote a pair of the stable CHF=C=CHF enantiomers, which may be the initial or final state of the related internal rotation process, and *cis*-TS and *trans*-TS denote the TS in the process. Although the MO irreducible representations are denoted by the point group ($C_{2v}$ or $C_{2h}$) *cis*-TS or *trans*-TS belongs to, we link the same first label (A or B) in the irreducible representations in the figure. The bonding OMO's and the anti-bonding VMO's are separated with a horizontal double line. It is notable that no correlation lines cross the double line, i.e. the NB(non-bonding)MO level, and so all of them are symmetry allowed no matter what the IRC path is.

However, MO correlation lines may cross through the *cis*- or *trans*-IRC process. If the line crosses between P and TS, then it must also cross between R and TS, i.e. crossing twice. If we ignore TS, the direct correlation lines will not cross, as shown in the left-hand column of Fig. 17. If twice crossing took place between OMO and VMO, it would be symmetry forbidden, which could not appear in the stable MO direct correlation diagram.

## 4 Approximate symmetry characteristics of allene 1,3-fluor-chloride

We may use CHF=C=CHCl as a prototype model for allene-1,3-dihalides with different halogen atoms. This molecule also has two stable optical enantiomers, which may transform to each other through the internal rotation about the C=C=C axis.

For the stable molecular configuration at AM1 level, the CHF group planes at two sides of the molecule are orthogonal roughly, and the CCC axis is linear approximately. The symmetry and approximate symmetry of the TS and various IRC states for CHF=C=CHCl through the internal rotation process may be analyzed in the same fashion as CHF=C=CHF. Since one fluorine atom is replaced by a chlorine atom, the symmetry of CHF=C=CHCl drops compared with CHF=C=CHF.

For CHF=C=CHCl, the internal rotation chiral transition may also be realized through the *cis*- or *trans*-IRC path in connection to the *cis*- or *trans*-TS, which is a planar molecule. Different from CHF=C=CHF, the TS of CHF=C=CHCl has the molecule plane as is only symmetric element, so it belongs to $C_S$ point group. On the other hand, CHF=C=CHCl does not keep any nontrivial common point symmetry in the internal rotation. The related membership function is less one due to both the space factor and the intrinsic factor which should be the main control factors of symmetry selection rules of the related chemical process. Here we analyze the symmetry and the approximate symmetry in relation to $C_2$ symmetric transformation.

For CHF=C=CHCl, through the internal rotation process the membership function in relation to $C_2$ transformation is usually less one. It must be pointed out that here the less one membership function is mainly due to the intrinsic rather than space factor. Since now $C_2$-axis is an approximate symmetry element, so it may be chosen by different ways. How do we analyze the symmetry element (e.g., $C_2$-axis) and corresponding Cartesian coordinate system? For CHF=C=CHF, we set the coordinate origin at the midpoint of C(2)C(3), the line connecting C(1) and origin as $Z$-axis, i.e. the $C_2$-axis, and the line connecting C(2)C(3) and the line perpendicular to the CCC plane through the origin as $Y$- and $X$-axis, respectively. In CHF=C=CHF, owing to CCC composing an isosceles triangle, the height, angular bisector and the median are the same, but this is not true for CHF=C=CHCl. Owing to the orthogonality of the Cartesian coordinate axes, the origin will be chosen at the pedal point, which is necessary and convenient for analyzing the LCAO($p_x, p_y$ and $p_z$)-MO. As the standard orientation in Gaussian program ignores the approximate symmetry, the orientation was transformed to the above chosen coordinate system for adapting the $p$-AO's direction.

For both CHF=C=CHF and CHF=C=CHCl, through the internal rotation the molecule will experience the optical chiral transition, an isomerization between the enantiomers. In this process, the curve of energy (vs.) IRC would be symmetric about the TS point. The TS of CHF=C=CHCl should belong to $C_S$ group, while the other states only to $C_1$, no non-trivial symmetry indeed. These two point groups include the following symmetric transformations:

$$C_1 : G_{IRC} = \{\hat{E}\} \tag{16a}$$

$$C_S : G_{TS} = G_{IRC} \cup G'_{TS} = \{\hat{E}\} \cup \{\hat{M}\} = \{\hat{E}, \hat{M}\} \tag{16b}$$

where $G'_{TS} = \{\hat{M}\}$ is the symmetric transformation set of the TS only, and $\hat{M}$ is the mirror reflection. Certainly, for the *cis*-IRC and *trans*-IRC, $\hat{M}$ should be different. Although both mirrors are the TS molecular plane, the *cis*-TS mirror includes the fuzzy two-fold axis ($\underset{\sim}{C}_2$), whereas the *trans*-TS mirror would be orthogonal to $\underset{\sim}{C}_2$.

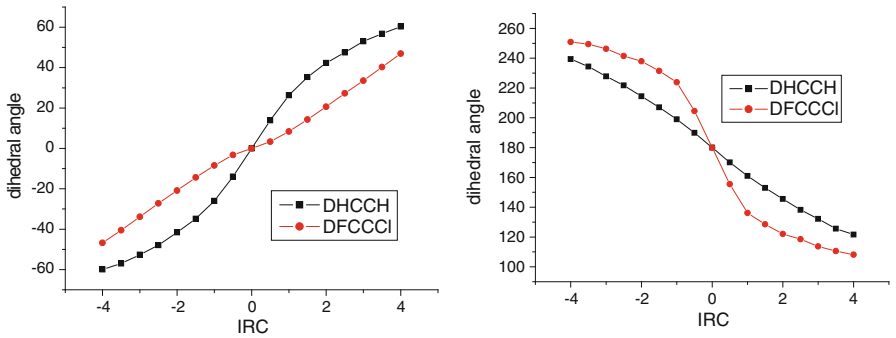


**(a)** *cis*-IRC **(b)** *trans*-IRC

**Fig. 18** AM1 Dihedral angles (vs.) IRC for the internal rotation of CHF=C=CHCl through the *cis*-IRC (**a**) and *trans*-IRC (**b**) paths; *black* and *red lines* correspond to the two kinds of dihedral angles. (Color figure online)

For the IRC states other than TS, the space relationship between the fuzzy mirror and $C_{\sim 2}$ is maintained in TS. For CHF=C=CHCl, the IRC states other than TS do not belong to any point group, but they may have the joint symmetry of $\hat{\mathrm{R}}\hat{\mathrm{M}}$, where $\hat{\mathrm{R}}$ and $\hat{\mathrm{M}}$ are the reaction reversal and reflection, respectively. The corresponding symmetric transformation group is:

$$G(\mathrm{RM}) = \{\hat{\mathrm{E}}, \hat{\mathrm{R}}\hat{\mathrm{M}}\} \tag{17}$$

Of course, for the *cis*-IRC and *trans*-IRC, their own $\hat{\mathrm{R}}$ and $\hat{\mathrm{M}}$are both different; they may be denoted as follows:

$$\mathrm{G(RM)}_C = \{\hat{\mathrm{E}}, \hat{\mathrm{R}}_\mathrm{c}\hat{\mathrm{M}}_\mathrm{YZ}\} \tag{17a}$$
$$G(\mathrm{RM})_T = \{\hat{\mathrm{E}}, \hat{\mathrm{R}}_\mathrm{t}\hat{\mathrm{M}}_\mathrm{XY}\} \tag{17b}$$

At AM1 level, through the *cis*-IRC and *trans*-IRC paths, the variation of molecular configuration will be similar for CHF=C=CHCl and CHF=C=CHF, and the bond length and bond angle variation will be small. Through the internal rotation, the main variation should be in dihedral angles, as shown in Fig. 18 for CHF=C=CHCl through the two IRC paths.

Figure 19 shows the energy of CHF=C=CHCl versus *cis*- and *trans*-IRC. These curves in the diagram are symmetric about the TS. The states with the opposite IRC values can be regarded as a pair of optical enantiomers. Comparing with the bond length, bond angle and dihedral angle in the internal rotation of CHF=C=CHF through the *cis*-IRC and *trans*-IRC paths and that of CHF=C=CHCl, we find that the variation is similar in the dihedral angle. In the dihedral angle (vs.) IRC curve, there is the inversion symmetry about TS. The maximum for the potential energy (vs.) IRC curves locates at the TS, and from this point, the potential energy drops symmetrically along two directions (reagent and product) as shown in Figs. 12 and 19. However, for the isomerization process of these two molecules, the variations are much different. For

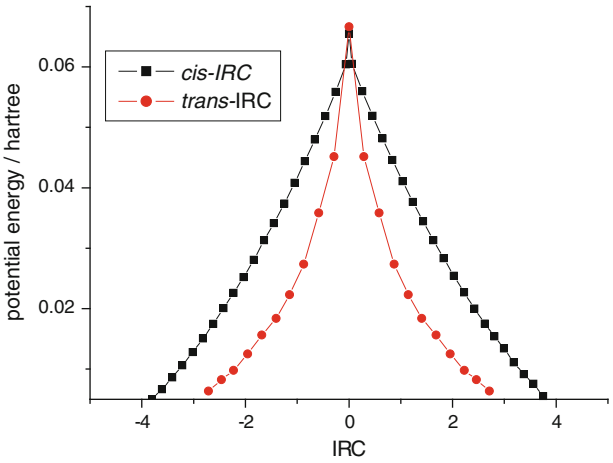


**Fig. 19** The energy (vs.) IRC diagram for CHF=C=CHCl through the *cis*-IRC (*black*) and *trans*-IRC (*red*) internal rotation at AM1 level. (Color figure online)

CHF=C=CHF, its TS has well-defined symmetry of $C_{2V}$ or $C_{2h}$ point group, while the states other than TS have well-defined symmetry of $C_2$ point group. On the other hand, for the CHF=C=CHCl process, all IRC states include the TS have no $C_2$ symmetry, so we may only analyse their approximate symmetry.

It is notable where the approximate symmetry in relation to $\underset{\sim}{C}_2$ group is introduced owing to the difference between Cl atom and F atom, the intrinsic factor rather than the space factor. In general, the intrinsic factor will be more important in chemistry.

### 4.1 The membership functions in relation to $\hat{R}\hat{M}$

Through the whole internal rotation process, CHF=C=CHCl has only well-defined $\hat{R}\hat{M}$ symmetry. Of course, the $\hat{R}$ and $\hat{M}$ of the *trans*-IRC path are different from those of the *cis*-IRC path. The $\hat{R}$ may be denoted as $\hat{R}_t$ and $\hat{R}_c$ in reaction to the *trans*-IRC and *cis*-IRC paths, respectively. The $\hat{M}$ denotes as the mirror reflection, corresponding to the well-defined symmetry of the TS, and in the *trans*-IRC and *cis*-IRC process, the mirrors are XY- and YZ-coordinate planes, respectively, and so the corresponding $\hat{M}$ are accordingly denoted as $\hat{M}_{XY}$ and $\hat{M}_{YZ}$. The calculation in relation to $\hat{R}\hat{M}$ was related to states with the opposite IRC-values. On the other hand, although the Gaussian calculation may include some symmetry conditions related to the point groups, but not those to $\hat{R}\hat{M}$.

In the internal rotation process, a single-point state may include 22 MO's, and at AM1 level, each MO ($\psi_\rho$) is expressed as the LCAO of the 22AO's ($\phi_i$) of the seven atoms,

$$\psi_\rho = \Sigma_i a_i \rho \phi_i \ (\rho, i = 1, 2, \ldots, 22) \tag{18}$$

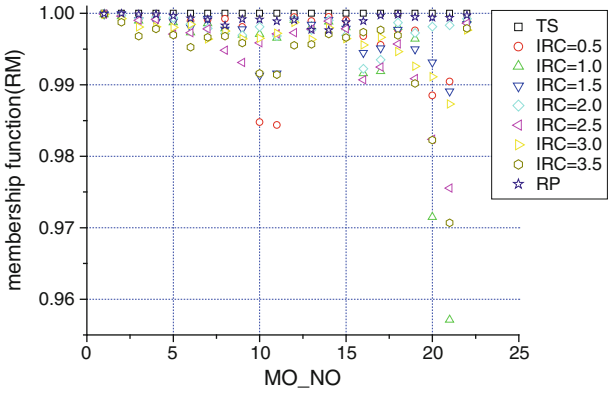


**Fig. 20** The MO membership functions in relation to the joint symmetric transformation $\hat{R}\hat{M}$ (at AM1 level) for CHF=C=CHCl through the internal rotation with the *cis*-IRC path. The MO numbering accords with the MO energy order. TS–the transition state; RP–the stable molecules. For the states with the opposite IRC-values, the membership functions are the same

For the MO $\psi_\rho$, the AO criterion may be denoted as [12–16],

$$Y_i = a_i \rho a_i \rho^* / \Sigma_j a_j \rho a_j \rho^* \tag{19}$$

Using the normalized MO LCAO coefficient, the denominator $\Sigma_j\, a_j \rho a_j \rho^*$ equals one. For MO $\psi_\rho$, the membership function of transformation $\hat{G}$ is,

$$\mu\left(\hat{G};\psi_\rho\right) = \Sigma_i Y_i \wedge Y_{Gi} \tag{20}$$

It is notable that for Eq. (20), space factor $\varphi$(GJ,G$^{\#}$J) would approach one, i.e. for any J-atom in relation to $\hat{G}$, G$^{\#}$J-atom and GJ-atom must be close or coincide. When $\hat{G}$ is $\hat{R}$ or $\hat{R}\hat{M}$, this equation may be wrong if the space factor does not approach one. However if $\hat{G}$ is $\hat{R}\hat{M}$, Eq. (20) will be true. Using this equation, for MO of CHF=C=CHCl, the membership functions related to $\hat{R}\hat{M}$ may be obtained without symmetric restriction in the whole rotation process. Figure 20 shows the results of the *cis*-IRC path at AM1 level. The $\hat{R}\hat{M}$ membership functions are close to one as most of them between 0.99 to 1. We may consider that these MO's have well-defined symmetry of this joint transformation, and the slight deviation from 1 may be a result of the approximation of our calculation. For the *trans*-IRC path, we may analyze similarly. The results are even better than those of the *cis*-IRC path.

It is noteworthy that through the internal rotation, the MO's of CHF=C=CHF have well-defined symmetry of G($R_cC_{2v}$) or G($R_tC_{2h}$) group, but the MO's of CHF=C=CHCl have only well-defined symmetry related to the subgroup of these groups:

$$G(RM)_C = \{\hat{E}, \hat{R}_c\hat{M}_{YZ}\} \subset G(R_cC_{2v}) \tag{21a}$$

$$G(RM)_T = \{\hat{E}, \hat{R}_t\hat{M}_{XY}\} \subset G(R_tC_{2h}) \tag{21b}$$

Since there is no well-defined $C_2$ symmetry in the internal rotation of CHF=C=CHCl, the irreducible representation analysis of the MO's is more difficult.

### 4.2 MO fuzzy correlation diagram in relation to $\hat{C}_2$ transformations

In the whole internal rotation of CHF=C=CHF, $C_2$ symmetry remains, so the membership functions of all MO's should equal one and the irreducible representation is the pure, i.e. either symmetric (g) or anti-symmetric (u). However, in the process of CHF=C=CHCl, there is only approximate symmetry related to $C_2$. The approximate symmetry stems from the intrinsic factor related to the difference between fluorine and chlorine atoms while the space factor is less important. Therefore, for the MO's, we may analyze the irreducible representation component related to $C_2$. For MO in Eq. (18), the coefficient, $a_{i\rho}$ may be decomposed into to g and u parts,

$$a_{i\rho} = a_{i\rho}(g) + a_{i\rho}(u) \tag{22}$$

The symmetric (Xg) and anti-symmetric (Xu) components for the MO's can be defined as follows,

$$Xg = \Sigma a_{i\rho}^2\,(g) \tag{22a}$$

$$Xu = 1 - Xg = \Sigma\, a_{i\rho}^2\,(u) \tag{22b}$$

The components of MO's of the TS, reagent and product (R & P) may be calculated at the AM1 level. Figure 21 shows the related fuzzy MO correlation diagram in relation to Xg. As Xg is more than 0.5, the related MO will be mainly symmetric, and as Xg is less than 0.5 the related MO will be mainly anti-symmetric, belonging to B irreducible representation of $C_2$ group.

As shown in Fig. 21, from Xg values, we may note the main-representation [14,15] with MO symbols. When Xg near 0.5, the MO symmetry in relation to $\hat{C}_2$ is not clear, and the related membership function will be very small. The related symmetry restriction may be ignored. Xg values of every MO's for P and R appear to be approximately the same as expected for a pair of enantiomers. In the figure, the black lines denote the common cases with the same main-representation, while the red lines denote minor MO correlation lines with different main-representations. In a red line at least one MO has an Xg value close to 0.5, i.e. in 0.4 to 0.6.

The correlation lines link two MO's with the same main irreducible representation according to the energy order. The MO may just belong to one irreducible representation; it may also belong to a combination of two. In the combination, the major component is called the main-representation [15]. In the fuzzy correlation diagram, the main-representation symbol is used to replace the pure representation arranged in the MO energy order. According to this classification, there are 10 A and 12 B in the 22 MO's of P or R considered. However, the main-representations (A and B) numbers for the 22 MO's of the TS may be different from that of the stable molecules P and R. For a certain MO, when Xg $\approx$ 0.5 and Xu $\approx$ 0.5

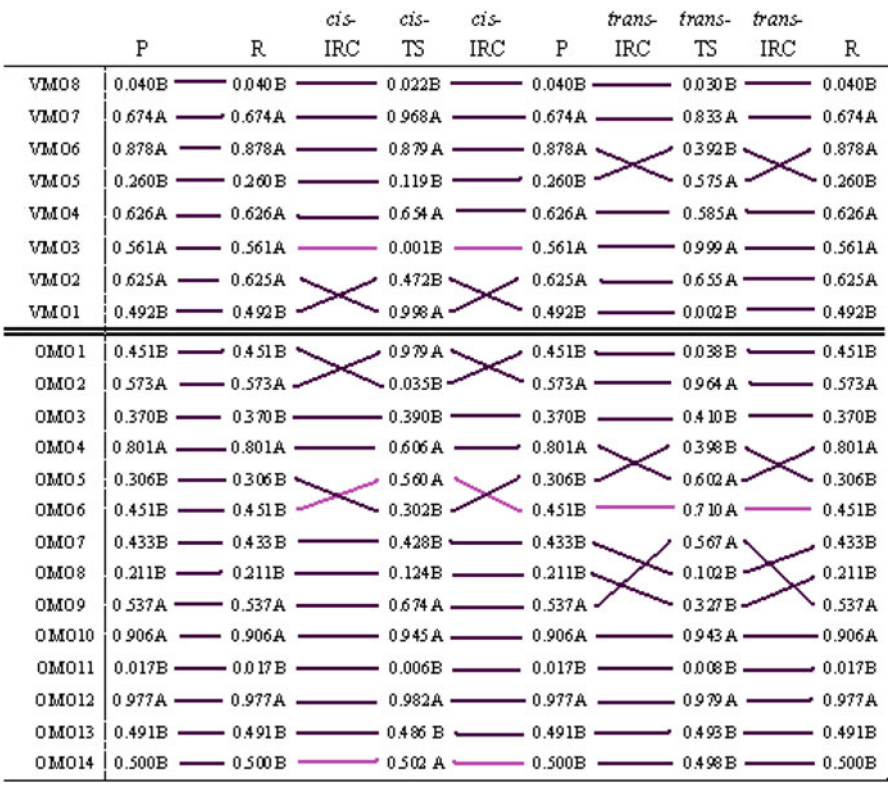


**Fig. 21** The orbital fuzzy correlation diagram of CHF=C=CHCl in relation to $\hat{C}_2$ in the internal rotation process at AM1 level

occur, the related membership function should be small, and the corresponding main-representation will be hard to assign. For example, the membership functions of OMO14 of P, R and TS related to $\hat{C}_2$ are only about 0.001 to 0.002, and that of OMO13 is only about 0.02. Therefore, for MO with Xg $\approx$ 0.5 (0.4–0.6), the next main-representation may be used and to determine the fuzzy correlation line [10, 11].

As shown in Fig. 21, certain MO fuzzy correlation lines of the transition between TS and P (or R) cross, but they do not cross between OMO and VMO. Therefore, all related processes are the approximate symmetry allowed. If OMO and VMO cross, e.g., HOMO and LUMO, the relevant process would be forbidden. In addition, through the *trans*-IRC and *cis*-IRC, the relationships of the TS and P and those of TS to R are symmetric, i.e. as there are correlation lines cross between P and TS, then there must be another lines cross between the TS and R. There is, however, no direct cross between P and R correlation lines, as shown in the first column on Fig. 21. If such cross appear between lines of OMO and VMO, e.g., HOMO and LUMO, the process would be symmetry forbidden, which cannot be determined directly in the MO correlation diagram between P and R without TS.

Different from CHF=C=CHF, CHF=C=CHCl in the internal rotation has no well-defined symmetry $C_2$, it only has approximate symmetry. The fuzzy representation for a MO is defined as follows,

$$\mathrm{XgA} + \mathrm{XuB} = \mathrm{XgA} + (1 - \mathrm{Xg})\mathrm{B} \tag{23}$$

which is not a pure representation, and whose membership function is less one, even for MO's of the TS due to the intrinsic factor introduced by replacing a F atom by a Cl atom. As shown in Fig. 21 , component Xg (or Xu) related to $\hat{C}_2$ of P and R MO's seems to be symmetric about the TS.

To start with, we consider the *trans*- and *cis*-IRC process. The component Xg (or Xu) of some OMO's far from the HOMO, e.g., OMO13 and OMO14 (Fig. 21), related to $\hat{C}_2$ is close to 0.5, and their membership functions are small. As the two MO's are LCAO's of C=CHCl and C=CHF fragments, whereas in CHF=C=CHF, OMO13 and OMO14 are those of two C=CHF fragments, and are degenerate with pure representations (S, Xg = 1 or A, Xg = 0), see Fig. 17.

Now we examine the variation of allene-1,3 fluor-chloride with the *cis*-IRC path. By means of the Gaussian program, the internal coordinate configurations of the IRC path are the results without the any symmetry restriction condition. Though the deviation of MO's in relation to the $\hat{R}\hat{M}$ union transformations perfect symmetry much less, as shown in Fig. 20, however using the Gaussian program we can not get the reaction path according to the symmetry restriction condition in relation to the $\hat{R}\hat{M}$ union transformations, directly. Utilizing the Gaussian program, we can get the internal coordinate configurations about various IRC values without any symmetry restriction condition. For a pair of the skeleton internal coordinate configurations with the certain opposite *cis*-IRC values, we can get them only without any symmetry restriction condition, from Gaussian program, respectively. However, owing to these two configurations are enantiomorphous, we can get the internal coordinate configurations with the symmetry restriction condition in relation to the $\hat{R}\hat{M}$ union transformations by means of the furthermore calculation. For the various skeleton internal coordinate configurations, it will be single-point calculated, point-by-point, and to get the relative approximate symmetric parameters, the membership functions and symmetric representation components Xg of various MO's. The Fig. 22 shows that through the *cis*-IRC internal-rotation process, the membership functions and the symmetric representation components Xg in relation to fuzzy two-fold rotation transformation of the CHF=C=CHCl MO's (vs.) the IRC diagram. It seems that for more MO's in relation to the $\hat{C}_2$transformations the variation of membership functions and Xg values (vs.) IRC relative curves are symmetric about TS. It ought to be noted that as the calculation without the symmetry restriction condition in relation to the $\hat{R}\hat{M}$union transformation, the relative symmetry about TS will be screened. The similar results of *trans*-IRC cases are omitted, for save the space.

Owing to such approximate symmetry will be produced from the intrinsic factor, the MO membership function ought to be connected with the MO irreducible representation components, and that is much difference for various MO's. Comparing with the space factor, the space factor effect for various MO's ought to be the similar.

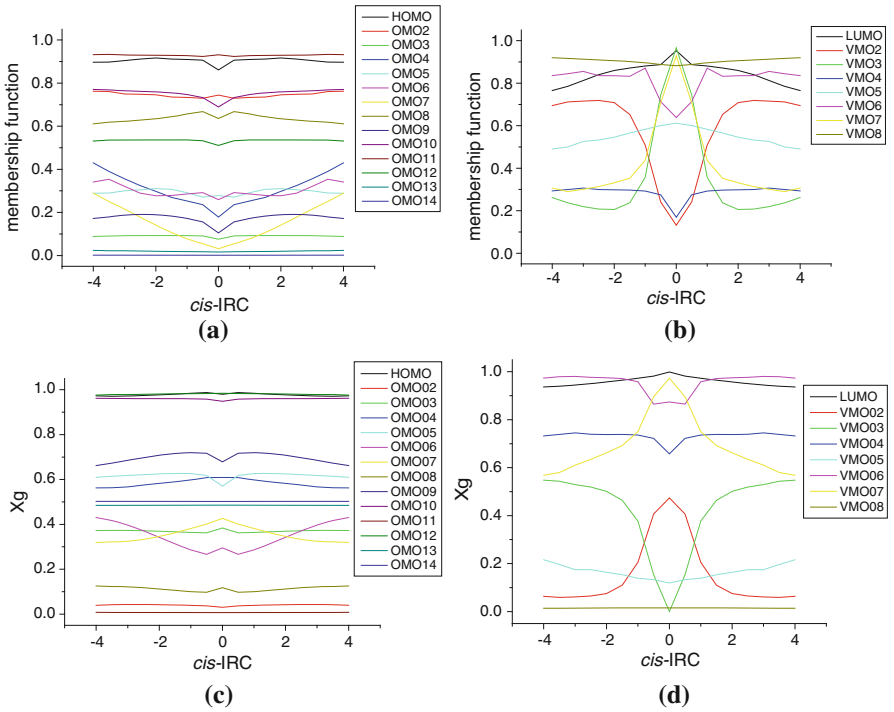


**Fig. 22** Through the *cis*-IRC internal-rotation process, the membership functions (**a, b**) and the symmetric representation components Xg (**c, d**) in relation to fuzzy two-fold rotation transformation of the CHF=C=CHCl MO's (vs.) the IRC digraim. **a** The membership functions of some OMO's. **b** The membership functions of some VMO's. **c** The symmetric representation components of some OMO's. **d** The symmetric representation components of some VMO's

## 5 Approximate symmetry characteristics of other allene-1,3-dihalides

After examining CHF=C=CHF and CHF=C=CHCl, the two prototypical CHX=C=CHY with the same and different halogen, we come to analyze the approximate symmetry characteristics of other CHX=C=CHY through the internal rotation chiral transformation process briefly. Here we only analyze (fuzzy) correlation diagrams, membership functions and MO representation components related to $\hat{C}_2$ of the TS and stable state molecule of allene-1,3-dihalides.

### 5.1 The membership functions and representation components about $\hat{C}_2$

For the 22 MO's in the valance shell of CHX=C=CHY are calculated at AM1 level. Figures 23 and 24 show the symmetric representation components (Xg) and membership functions of frontier and near frontier MO's, respectively. In these figures, each column separated by vertical dot-lines represent four CHX=C=CHY molecules with one common halogen atom, and X denotes, from left to right, F, Cl, Br and I in such order turn.

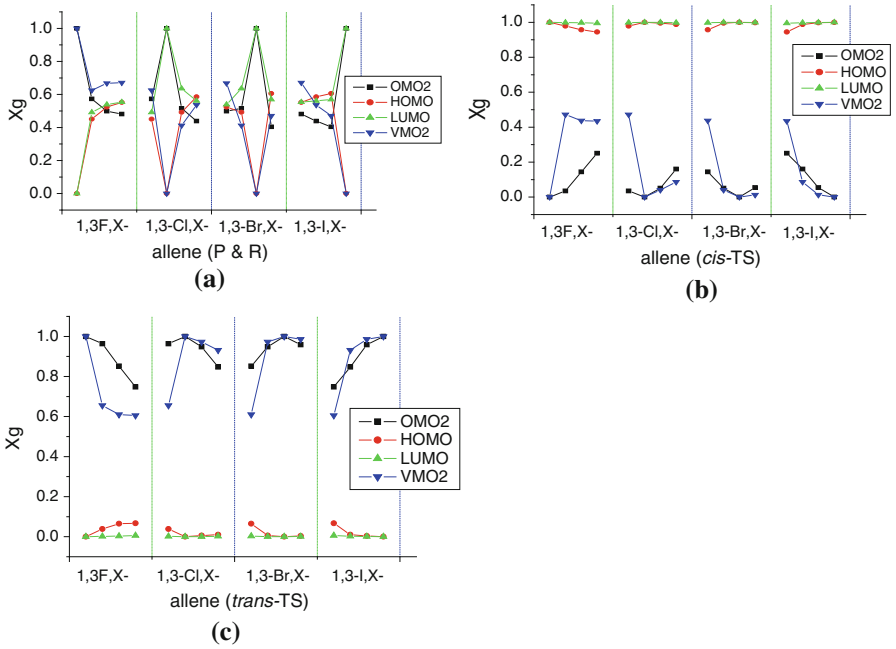


**Fig. 23** The symmetric representation components (Xg) of allene-1,3-dihalides MO's related to $\hat{C}_2$ for **a** stable molecules (P and R), **b** *cis*-TS, **c** *trans*-TS and X stands for F, Cl, Br, and I in that order in each column

When the two halogen atoms are the same, all of the related TS and stable molecules should have well-defined symmetry of $C_2$. For these species, Xg of the MO's should be either 0 or 1, and the membership functions must be 1. Figures 23 and 24 show the prototypical results. When the two halogen atoms are different, both MO Xg and membership function are between 0 and 1 as shown in the two figures. As mentioned above, this is also true for other MO's. As X and Y are different, six CHX=C=CHY molecules exist. Related MO's in the stable molecules, and (*cis*- and *trans*-) TS of the six CHX=C=CHY molecules along with the relationship of membership function versus representation component are shown in Fig. 25, where BV denotes the boundary value as the curve shown in Fig. 11. As shown in Fig. 25, all the points locate above the boundary values. Although the points appear to group near the boundary value curve, they also scatter.

## 5.2 MO fuzzy correlation diagram related to $\hat{C}_2$

Figure 26 shows the MO correlation diagram of allene-1,3-dihalides (CHX=C=CHX, X=F, Cl, Br, I) according symmetry$\hat{C}_2$, which remains through the whole rotation process, for two stable molecules P and R, and two TS (*cis*- and *trans*-TS). As shown in the Figure, the MO irreducible representation symbols of (P and R), *cis*-TS, and *trans*-TS correspond to those of point group $C_2$, $C_{2v}$ and $C_{2h}$, respectively. All these

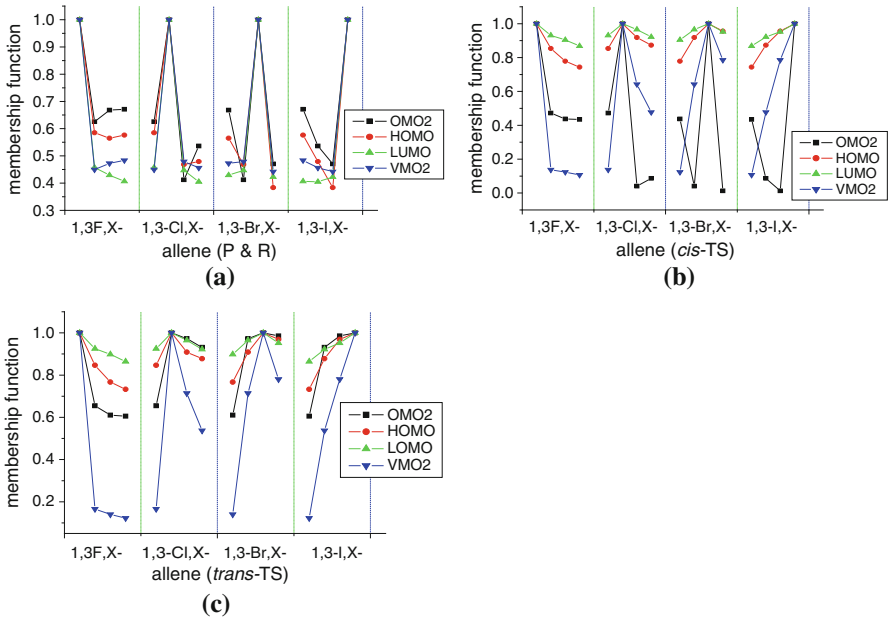


**Fig. 24** Membership functions of allene-1,3-dihalides MO related to $\hat{C}_2$ for **a** stable molecule (P and R), **b** *cis*-TS, **c** *trans*-TS, and X stands for F, Cl, Br, and I in that order in each column

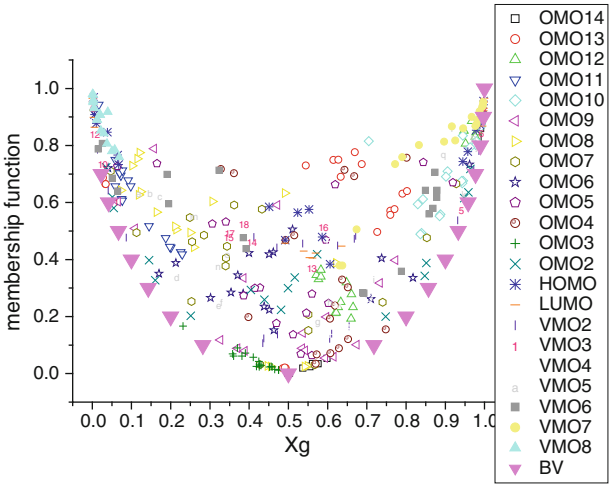


**Fig. 25** Relationship of MO membership function (vs.) representation component related to $\hat{C}_2$ for the internal rotation of allene-1,3-dihalides

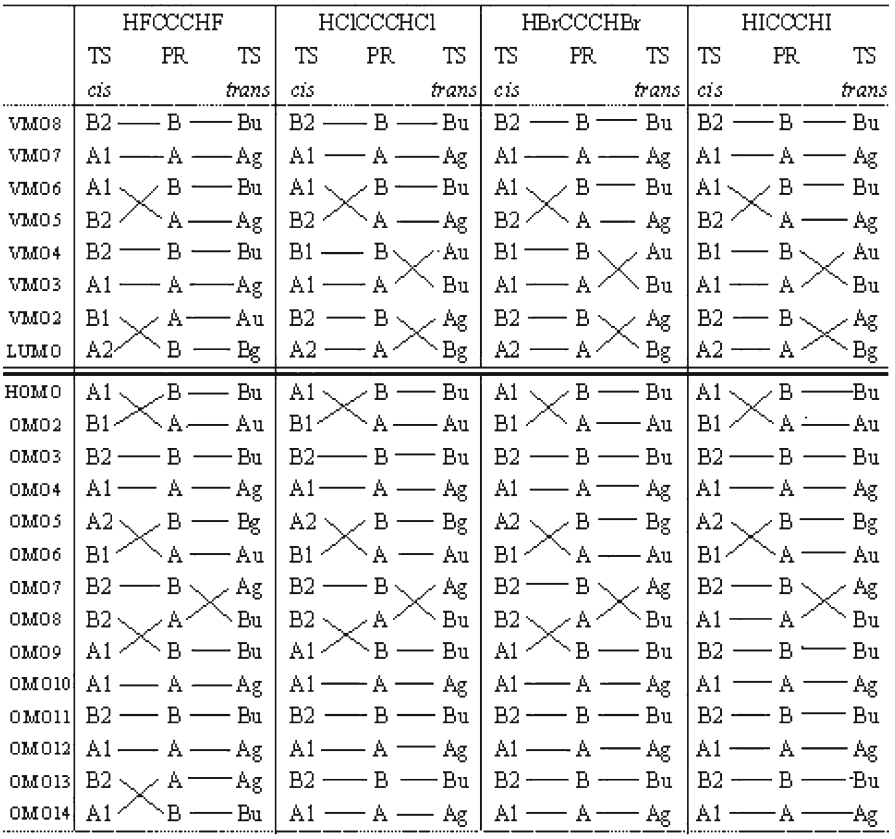


**Fig. 26** MO correlation diagram for allene-1,3-dihalides with the same halogen (F, Cl, Br and I) through the internal rotation process related to $\hat{C}_2$

representations are pure. Since all the molecular systems always maintain the well-defined $C_2$ symmetry, we only need to consider the first label in the irreducible representation symbols, that is, A or B when we correlate the MO in the figure. The correlation lines only cross between OMO's or between VMO's, whose processes would be symmetry allowed, but not between OMO and VMO. Of course, as the cross occurs, it does twice, first between P and TS, and then between TS and R, as mentioned for CHF=C=CHF shown in Fig. 17.

For CHX=C=CHY with different X and Y, no well-defined symmetry related to $\hat{C}_2$ exists, so only approximate symmetry presents. The relative fuzzy symmetric point group and the fuzzy representation have been shown in Eqs. (7) and (8), respectively. For MO's, they are expressed by membership function ($\mu$) and representation component (Xg or Xu). The MO representation in the fuzzy correlation diagram will be replaced by the main-representation of the MO. Figures 27 and 28 present the fuzzy correlation diagrams of stable (P and R) (vs.) TS of six CHX=C=CHY species (X≠Y, X,Y=F, Cl, Br, I) through the internal rotation process.

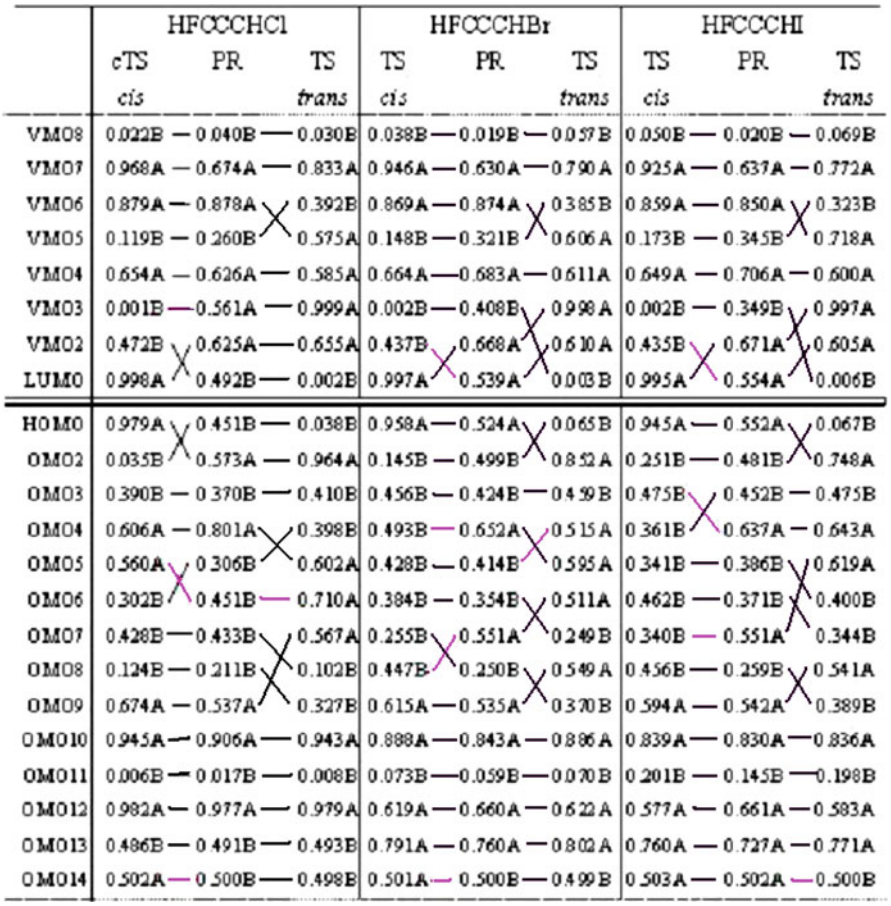


**Fig. 27** MO fuzzy correlation diagram for allene-1,3-dihalides with different halogen atoms (F and Br or Cl or I) through the internal rotation process in relation to $\hat{C}_2$

In these Figures, the number value before the MO main-representation (A or B) denotes its symmetric representation component Xg. When Xg is larger than 0.5, the main-representation is A; otherwise the main-representation is B. The most correlation lines denote the MO's with the same main-representation are, while a few correlation lines denote the minority MO's with different main-representations. On these few correlation lines, at least one correlated MO has an Xg close to 0.5 (e.g., 0.4 to 0.6). Since the MO correlation lines of stable molecules P and R are symmetric about the TS, they are analyzed jointly. The correlation lines do not cross the NBMO level, nor do they cross between OMO and VMO, and so these processes should be symmetry allowed. The correlation degree of two MO's linked by the fuzzy correlation line, and the forbidden process involved in the fuzzy correlation diagram will be examined in our further work.

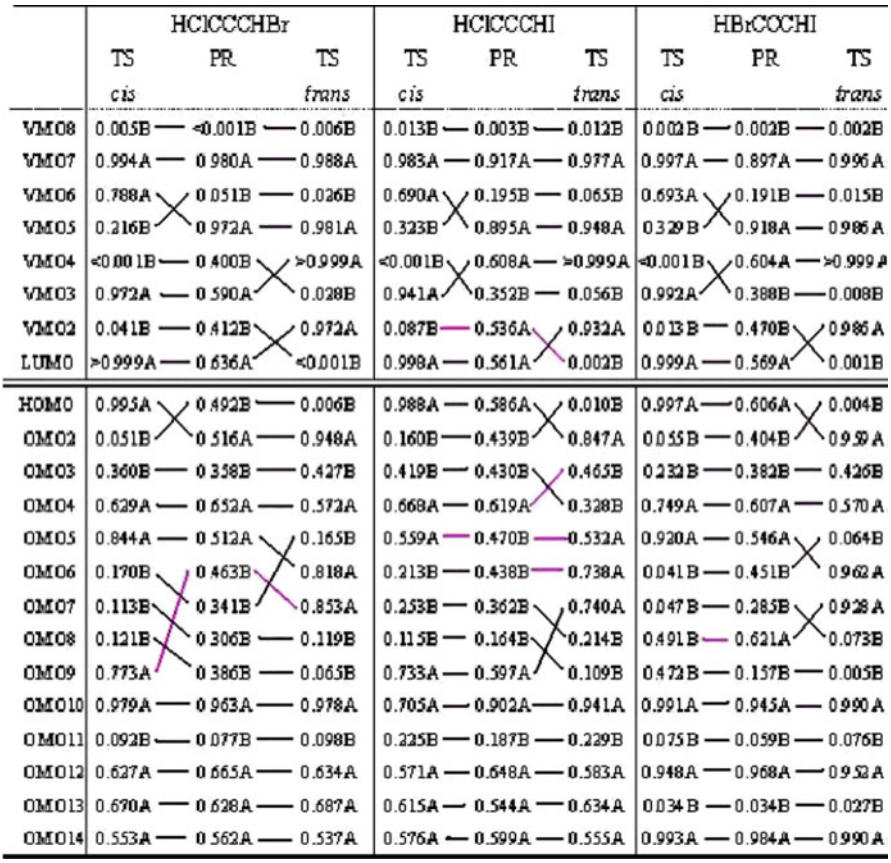


**Fig. 28** MO fuzzy correlation diagram for allene-1,3-dihalides with different halogen atoms (other than F) through the internal rotation process in relation to $\hat{C}_2$

## 6 Conclusions

In this paper, we examined the approximate symmetry characteristics for the chiral transition of allene-1,3-dihalides through the internal rotation at AM1 level. The *cis*-IRC and *trans*-IRC paths were considered. In the two IRC dynamic ways, the related approximate symmetry characteristics are different. For allene-1,3-dihalides with the same or different halogen atoms, related approximate symmetry characteristics are also different. The main conclusions include:

1. Through the *cis*-IRC or *trans*-IRC internal rotation path of allene-1,3-dihalides with the same halogens, both TS are planar. The related *cis*-TS and *trans*-TS have well-defined symmetry of $C_{2v}$ and $C_{2h}$ group, respectively. However, other *cis*-IRC and *trans*-IRC states have only well-defined symmetry of $C_2$ group, and they have only approximate symmetry related to $C_{2v}$ and $C_{2h}$.
2. The *cis*-TS and *trans*-TS of allene-1,3-dihalides with different halogen atoms well-defined symmetry of $C_s$ point group. Other *cis*-IRC and *trans*-IRC states have no

well-defined symmetry in relation to any non-trivial common point group, and they have only approximate symmetry in relation to $C_2$ group. In the whole *cis*-IRC or *trans*-IRC process, among the molecular internal-coordinate parameters, only dihedral angles changes significantly.

3. For the approximate symmetry system, the space factor and the intrinsic factor make the membership function to decrease. For the MO's of a certain molecule, the space factor is similar, but the intrinsic factor will be very different. In chemistry, the intrinsic factor is more important.
4. For allene-1,3-dihalides with the same halogen atom, the membership functions decrease due to the space factor. This effect is similar for different MO's, and the decline of the MO symmetry cannot be ascribed to the overlap of different MO representation components.
5. The membership functions of allene-1,3-dihalides with different halogen atoms drop due to the intrinsic factor. This effect should be different for different MO's, and the drop of the MO symmetry may be ascribed to the overlap of different MO representation components.
6. For allene-1,3-dihalides, through a certain IRC internal rotation path, the states in the whole IRC process always have the well-defined symmetry of $G_{IRC}$ group.
7. For allene-1,3-dihalides with the same halogen atom, all *cis*-IRC and *trans*-IRC states have well-defined $C_2$ symmetry, according to which related MO correlation diagram was obtained. Occupied OMO's correlation lines and those of empty VMO's do not cross, and so the two IRC paths are symmetry allowed. If crossing appears, it must appear twice: one between TS and the reagent, and the other between TS and the product. For such cases, the related MO correlation diagram should also be examined those of TS, the reagent and product.
8. For allene-1,3-dihalides with different halogen atoms, through the *cis*-IRC and *trans*-IRC whole processes, we also obtained the MO fuzzy correlation diagram related to $C_2$.
9. The membership function and representation components are the two most important quantities in MO approximate symmetry analysis based on subset theory. Comparing to the study of MO's with well-defined symmetry, they are more closely related to symmetry group and to the irreducible representations, respectively. All MO membership function points locate above the boundary values in their plot versus irreducible representation components.

## References

1. P.G. Mezey, J. Maruani, Mol. Phys. **69**(1), 97–113 (1990)
2. P.G. Mezey, J. Maruani, Int. J. Quantum Chem. **45**, 177–187 (1993)
3. J. Maruani, P.G. Mezey, Compt. Rend. Acad. Sci. Paris (Série II) **305**, 1051–1054 (1987)
4. J. Maruani, A. Toro-Labbé, Compt. Rend. Acad. Sci. Paris (Série IIb) **323**, 609–615 (1996)
5. P.G. Mezey, Int. Rev. Phys. Chem. **16**, 361–388 (1997)
6. H. Zabrodsky, S. Peleg, D. Avnir, J. Am. Chem. Soc. **115**, 8278–8289, and references therein (1993)
7. D. Avnir, H. Zabrodsky, H. Hel-Or, P.G. Mezey, *Encyclopaedia of Computatational of Computational Chemistry*, vol. 4, ed. by Paul von Ragué Schleyer (Wiley, Chichester, 1998), pp. 2890–2901
8. P.G. Mezey, J. Math. Chem. **23**, 65–84 (1998)
9. R. Chauvin, J. Math. Chem. **16**, 245–256 (1994)

10. R. Chauvin, J. Math. Chem. **16**, 257–258 (1994)
11. X.Z. Zhou, Z.X. Fan, J.J. Zhan, et al., *Application of Fuzzy Mathematics in Chemistry*, Chap. 7. (National University of Defence Technology Press, Changsha Hunan, 2002), (in Chinese)
12. X.Z. Zhao, X.F. Xu, Acta Phys. Chim. Sci. **20**(10), 1175–1178 (in Chinese) (2004)
13. X.Z. Zhao, X.F. Xu, G.C. Wang, Y.M. Pan, Z.S. Cai, Mol. Phys. **103**, 3233–3241 (2005)
14. X.F. Xu, G.C. Wang, X.Z. Zhao, Y.M. Pan, Y.X. Liang, Z.F. Shang, J. Math. Chem. **41**(2), 143–160 (2007)
15. X.Z. Zhao, X.F. Xu, G.C. Wang, Y.M. Pan, Z.F. Shang, R.F. Li, J. Math. Chem. **42**(2), 265–288 (2007)
16. X.Z. Zhao, G.C. Wang, X.F. Xu, Y.M. Pan, Z.F. Shang, R.F. Li, Z.C. Li, J. Math. Chem. **43**(2), 485–507 (2008)
17. X.Z. Zhao, Z.F. Shang, G.C. Wang, X.F. Xu, R.F. Li, Y.M. Pan, Z.C. Li, J. Math. Chem. **43**(3), 1141–1162 (2008)
18. X.Z. Zhao, Z.F. Shang, H.W. Sun, L. Chen, G.C. Wang, X.F. Xu, R.F. Li, Y.M. Pan, Z.C. Li, J. Math. Chem. **44**(1), 46–74 (2008)
19. X.Z. Zhao, X.F. Xu, Z.F. Shang, G.C. Wang, R.F. Li, Acta Phys. Chim. Sci. **24**(5), 772–780 (2008)
20. K. Soai, T. Kawasaki, *Asymmetric Autocatalysis with Amplification of Chirality, in Topics in Current Chemistry* (Springer, Berlin, 2007), pp. 0340–1022
21. Y.S. Huang, J.H. Wu, J. Huaqiao Univ. (Natural Science) **22**(1), 40–43 (2001)
22. M.J. Frisch, G.W. Trucks, H.B. Schlegel, G.E. Scuseria, M.A. Robb, J.R. Cheeseman, V.G. Zakrzewski, J.A. Montgomery, Jr, R.E. Stramann, J.C. Burant, J.M. Dapprich, A.D. Daniels, K.N. Kudin, M.C. Strain, O. Farkas, J. Tomasi, V. Barone, M. Cossi, R. Cammi, B. Mennuggi, C. Pomelli, C. Adamo, S. Clifford, J. Ochterski, G.A. Petersson, P.Y. Ayala, Q. Cui, K. Morokuma, D.K. Malick, A.D. Rabuck, K. Raghavachari, J.B. Foresman, J. Cioslowski, J.V. Ortiz, A.G. Baboul, B.B. Stefanov, G. Liu, A. Liashenko, P. Piskorz, I. Komaromi, R. Gomperts, L.R. Martin, D.J. Fox, T. Keith, M.A. Al-Laham, C.Y. Peng, A. Nanayakkara, C. Gonzalez, M. Challacombe, P.M.W. Gill, B. Johnson, W. Chen, M.W. Wong, J.L. Andres, C. Gonzalez, M. Head-Gordon, E.S. Replogle, J.A. Pople, *Gaussian 98, Revision A.3* (Gaussian Inc., Pittsburgh, PA, 1998)
23. X.Z. Zhao, Z.S. Cai, G.C. Wang, Y.M. Pan, B.X. Wu, J. Mol. Struct. (THEOCHEM) **586**, 209 (2002)
24. X.Z. Zhao, *Application of Symmetry Principle in Field Theory to Chemistry*, vol. 106 (Science Press, Beijing, 1986) (in Chinese. CA), p. B38793f
25. R.B. Woodward, R. Hoffmann, Angew. Chem. **8**, 781 (1969)